ADVANCED MATERIALS
www.advmat.de

Improving the Stability of Metal Halide Perovskite Materials and Light-Emitting Diodes

*Himchan Cho, Young-Hoon Kim, Christoph Wolf, Hyeon-Dong Lee, and Tae-Woo Lee**

Metal halide perovskites (MHPs) have numerous advantages as light emitters such as high photoluminescence quantum efficiency with a direct bandgap, very narrow emission linewidth, high charge-carrier mobility, low energetic disorder, solution processability, simple color tuning, and low material cost. Based on these advantages, MHPs have recently shown unprecedented radical progress (maximum current efficiency from 0.3 to 42.9 cd A^{-1}) in the field of light-emitting diodes. However, perovskite light-emitting diodes (PeLEDs) suffer from intrinsic instability of MHP materials and instability arising from the operation of the PeLEDs. Recently, many researchers have devoted efforts to overcome these instabilities. Here, the origins of the instability in PeLEDs are reviewed by categorizing it into two types: instability of (i) the MHP materials and (ii) the constituent layers and interfaces in PeLED devices. Then, the strategies to improve the stability of MHP materials and PeLEDs are critically reviewed, such as A-site cation engineering, Ruddlesden–Popper phase, suppression of ion migration with additives and blocking layers, fabrication of uniform bulk polycrystalline MHP layers, and fabrication of stable MHP nanoparticles. Based on this review of recent advances, future research directions and an outlook of PeLEDs for display applications are suggested.

1. Introduction

Metal halide perovskites (MHPs) have stimulated intense research in the field of light-emitting diodes (LEDs), and researchers have achieved significant breakthroughs in the electroluminescence (EL) efficiency of MHP LEDs (PeLEDs) in only three years.[1–5] MHPs are semiconducting materials that have an ABX_3 perovskite crystal structure where A is an organic cation (e.g., methylammonium (MA) $CH_3NH_3^+$, formamidinium (FA) $CH(NH_2)_2^+$) or an alkali-metal cation (e.g., Cs^+, and partial doping of Rb^+ and K^+), B is a transition-metal cation (e.g., Pb^{2+}, Sn^{2+}), and X is a halide anion (Cl^-, Br^-, I^-). MHPs are suitable for the emission layers in LEDs because MHPs have: (i) a high photoluminescence quantum efficiency (PLQE) (up to 90% for $CsPbBr_3$ nanoparticle (NP) solution)[6], (ii) very narrow emission linewidth (full width at half maximum (FWHM) = 16.5 nm for $CsPbBr_3$),[7] (iii) high charge-carrier mobility (electron mobility $\mu_e \approx 1000\ cm^2\ V^{-1}\ s^{-1}$ for $CsPbBr_3$ single crystals,[8] 4500 $cm^2\ V^{-1}\ s^{-1}$ for $CsPbBr_3$ NPs[9]) comparable to that of Si ($\mu_e \approx 1000\ cm^2\ V^{-1}\ s^{-1}$),[10] and (iv) low energetic disorder (trap density $\approx 1.13 \times 10^9\ cm^{-3}$ for $FAPbBr_3$ single crystals,[11] Urbach energy = 15–30 meV[12,13]). Furthermore, low material cost, easy tuning of electronic properties (e.g., bandgap) by simple substitution of constituents, and applicability of diverse solution processes at low temperature (<100 °C) expand the potential of MHP emitters for applications in large-area displays. Particularly, a remarkably wide color gamut arising from the narrow emission linewidth of MHPs (FWHM < 20 nm) compared with those of organic emitters (FWHM ≈ 40 nm) and inorganic quantum dot (QD) emitters (FWHM ≈ 30 nm) is a distinct advantage of MHPs as alternative light emitters for vivid natural-color displays.

Dr. H. Cho
Department of Materials Science and Engineering
BK21 PLUS SNU Materials Division
for Educating Creative Global Leaders
Seoul National University
1 Gwanak-ro, Gwanak-gu, Seoul 08826, Republic of Korea
Dr. Y.-H. Kim, Prof. T.-W. Lee
Department of Materials Science and Engineering
Research Institute of Advanced Materials
BK21 PLUS SNU Materials Division
for Educating Creative Global Leaders
Seoul National University
1 Gwanak-ro, Gwanak-gu, Seoul 08826, Republic of Korea
E-mail: twlees@snu.ac.kr, taewlees@gmail.com
Dr. C. Wolf
Department of Materials Science and Engineering
Research Institute of Advanced Materials
Seoul National University
1 Gwanak-ro, Gwanak-gu, Seoul 08826, Republic of Korea
H.-D. Lee
Department of Materials Science and Engineering
Seoul National University
1 Gwanak-ro, Gwanak-gu, Seoul 08826, Republic of Korea
The ORCID identification number(s) for the author(s) of this article can be found under https://doi.org/10.1002/adma.201704587.

DOI: 10.1002/adma.201704587

Research on PeLEDs that can exhibit bright EL at room temperature began in 2014.[14,15] The EL efficiency was moderate (maximum current efficiency CE_{max} = 0.3[14] and 0.577 cd A^{-1}[15]), but these pioneering studies were enough to arouse intense interest among many researchers in the field of optoelectronics. In fact, early PeLEDs based on MHP emission layers were reported before 2014, but they showed bright EL only at cryogenic temperatures[16] or emitted from fluorescent organic dyes (leading to a broad EL with FWHM ≈ 90 nm), not from corner-sharing PbX_6 octahedra.[17] EL of PeLEDs that was barely detectable by the naked eye at room temperature was reported in 2011, but device efficiency could not be quantified because the brightness was too low.[18] The EL of PeLEDs at room temperature is limited due to: (i) thermal dissociation of excitons, (ii) slow bimolecular recombination caused by from spin–orbit coupling (Rashba effect) and anisotropy of organic A-site cations,[19,20] and (iii) the lack of optimal device structures for efficient charge-carrier injection and balanced transport of injected charge carriers. The thermal dissociation of generated excitons suppresses geminate radiative recombination and thus limits the luminescence efficiency. Also, large energy barriers between MHP emission layers and charge-injection/transport layers can reduce the efficiency of charge injection,[15] and charge unbalance in the emission layers can retard radiative recombination.[21]

The academic and technological background for fabricating efficient and bright PeLEDs has been established, along with developments of organic LEDs (OLEDs), QD LEDs, and MHP solar cells (PeSCs) over decades. The great progress in OLEDs and QD LEDs has provided effective strategies to construct efficient light-emitting devices and has yielded in depth understanding of the excited-state properties of light emitters.[22–26] Furthermore, recent intensive research on PeSCs has provided understanding of the electronic and structural properties of MHPs, and effective methods to control the morphology of MHP polycrystalline films.[27–29] Developments in these fields have revitalized studies of PeLEDs and significantly increased the EL efficiency and brightness.[14,15]

The recent rapid progress in EL efficiency of PeLEDs has been unprecedented; the record EL efficiency of visible PeLEDs steeply increased from CE_{max} = 0.3 to 42.9 cd A^{-1} (from maximum external quantum efficiency EQE_{max} = 0.1% to 8.53%) within one and a half years.[1] The EL efficiency of near-infrared PeLEDs also greatly increased from the initial efficiency (from EQE_{max} = 0.1%[14] to 10.4%[4] and 11.7%[5]). These achievements were based on diverse strategies to improve the luminescence properties of MHP emission layers and to facilitate charge-carrier injection and transport with a charge balance; these strategies include fabrication of uniform MHP polycrystalline layers,[1,7,30–32] grain-size engineering,[1,7] modifications of the crystal structure,[3,5,33] in situ preparation of MHP nanocrystal thin films,[4,34,35] suppression of luminescence quenching inside MHP layers[1] and at the interfaces with adjacent layers,[15] modifications of charge-injection/transport layers[7,15,30,36] and electrodes,[37,38] defect passivation,[39] and synthesis of colloidal MHP NPs.[30,40]

Despite these diverse approaches and solutions to improve EL efficiency, the industrialization and commercialization of PeLEDs are challenging due to the low stability of MHP materials and PeLEDs. Low stability of PeLEDs is mainly ascribed to intrinsic instability of MHP materials and instability arising from the operation of PeLEDs (**Figure 1**). Also, the low colloidal stability

Himchan Cho received his B.S. (February 2012) and Ph.D. (August 2016) in Materials Science and Engineering from the Pohang University of Science and Technology (POSTECH), Republic of Korea. He is currently working as a postdoctoral researcher in Materials Science and Engineering, BK21 PLUS SNU Materials Division for Educating Creative Global Leaders at the Seoul National University, Republic of Korea (September 2016 to present). His research interests include metal halide perovskites and their applications to optoelectronics.

Young-Hoon Kim received his M.S. (2014) from the Division of Environmental Science and Engineering and his Ph.D. (2016) in Materials Science and Engineering from the Pohang University of Science and Technology (POSTECH), Korea. He is currently working in Materials Science and Engineering at the Seoul National University, Korea as a postdoctoral researcher (2016–2017). His research focuses on solution-processed electronics based on organic and organic–inorganic hybrid materials for flexible displays and solid-state lightings.

Tae-Woo Lee is an associate professor in Materials Science and Engineering at the Seoul National University, Korea. He received his Ph.D. in Chemical Engineering from the KAIST, Korea in 2002. He joined Bell Laboratories, USA as a postdoctoral researcher and worked at Samsung Advanced Institute of Technology as a member of research staff (2003–2008). He was an associate professor in Materials Science and Engineering at the Pohang University of Science and Technology (POSTECH), Korea until August 2016. His research focuses on printed electronics based on organic and organic–inorganic hybrid materials for flexible displays, solid-state lightings, and solar-energy-conversion devices.

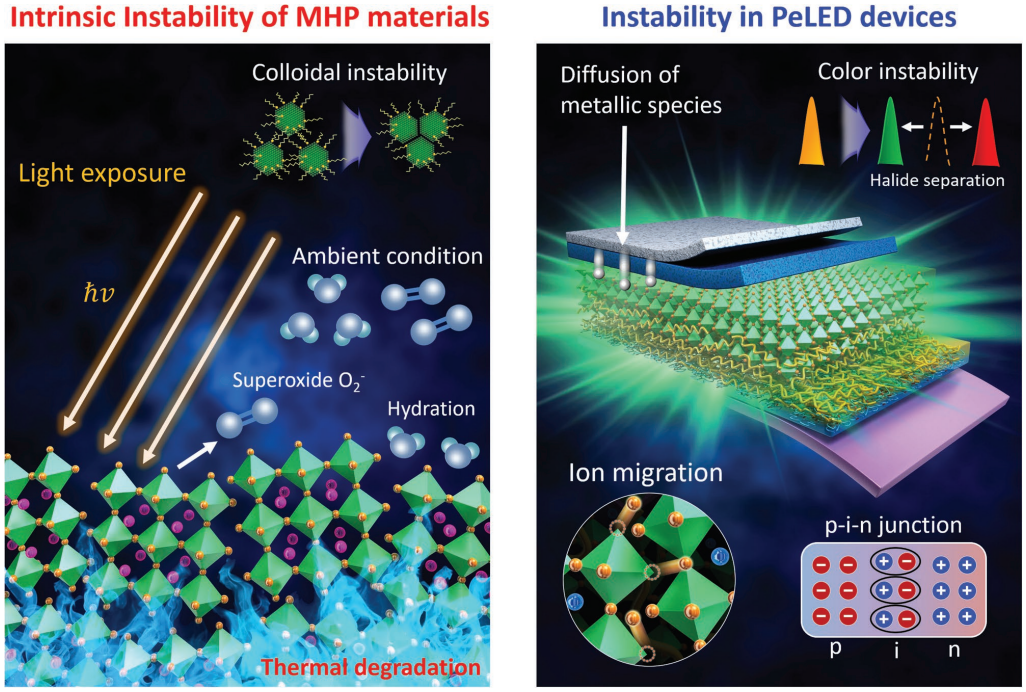

Figure 1. A schematic illustration describing the intrinsic instability of MHP materials and instability in PeLED devices.

of MHP NPs, which are frequently used for fabricating MHP emission layers, is another obstacle to be overcome before commercialization of high-stability PeLEDs is feasible.

To overcome the instability of PeLEDs, many researchers have devoted efforts to develop effective solutions; at this point, a full understanding of the origins of the low stability of PeLEDs and the possible solutions for stability problems is essential for designing further studies. Here, we review these factors that cause instability of MHP materials. We categorize the instability in PeLEDs into two types; i.e., instability of: (i) the MHP materials and (ii) the constituent layers and interfaces in PeLED devices. Then, we critically review recent studies that have tried to improve the stability of MHP materials and PeLEDs. Based on advances made in these studies, we present insight toward future research directions and an outlook of PeLEDs for practical applications.

2. Origins of the Low Stability of PeLEDs

2.1. Intrinsic Instability of MHP Materials

Many MHP materials undergo significant changes in structural and optoelectronic properties under phase transitions, thermal stress, air exposure, and illumination; some previous review papers have reported these instabilities of MHPs.[41–43] However, such reviews have mainly focused on applications of MHPs in solar cells. In this section, we review previous reports about the intrinsic instability of MHPs, with a focus on how this instability affects the luminescence properties of MHPs. Also, we review instability of MHP NPs in the solution and film states.

2.1.1. Influence of the Crystal Structure on Stability

MHPs can generally have three crystal structures: cubic, tetragonal, and orthorhombic, which can be transformed into each other reversibly by temperature change or chemical exchange of halide anions. The cubic perovskite structure is highly symmetric and thermodynamically more stable than the tetragonal and orthorhombic perovskite structures because of the lowest formation energy among three structures.[44,45] The structure of MHPs can be determined by calculating the tolerance factor

$$t_f = \frac{R_A + R_X}{\sqrt{2}\left(R_B + R_X\right)} \tag{1}$$

and the octahedral factor

$$o_c = \frac{R_B}{R_X} \tag{2}$$

where R_A, R_B, and R_X are the effective radii of the A, B, and X ions, respectively.[42,44,46,47] MHPs have cubic structure ($Pm3m$) when $0.813 \le t_f \le 1.107$ and $0.442 \le o_c \le 0.895$; otherwise it has a tetragonal ($I4/mcm$) or orthorhombic ($Pna2_1$) structure. Therefore, it is very important to control the radii of the constituent ions to make a stable cubic perovskite structure. Considering the effective radii of halogen anions (Cl^-: 167 pm; Br^-: 182 pm; I^-: 206 pm), $MAPbCl_3$ and $MAPbBr_3$ have cubic structure and $MAPbI_3$ has tetragonal structure at room temperature.[42,44,46–48] Due to the unstable tetragonal structure of $MAPbI_3$, $MAPbI_3$ PeSCs exhibit significant degradation at relative humidity (RH) ≥ 55%, whereas

$MAPb(Br_xI_{1-x})_3$ PeSCs retained their initial power conversion efficiency (PCE) for 20 d (at room temperature, RH = 55% for a day and 35% for the rest of days, without encapsulation) when $x \geq 0.2$ (cubic structure).[48]

2.1.2. Influence of Temperature on Stability

The MHP emission layer in PeLEDs must be thermally stable, because it may experience high temperatures during fabrication and device operation (Joule heating),[49,50] and because PeLEDs may be used outdoors.

The most frequently used A-site cation in MHPs is the MA^+ cation. Representatively, $MAPbBr_3$ and $MAPbI_3$ have been used as emission layers to fabricate high-efficiency green[1,34,35,37,39,51] and infrared[52] PeLEDs, respectively. However, under thermal stress, $MAPbX_3$ can suffer from severe degradation by the following decomposition pathways (P1) and (P2)[43,53–55]

$$CH_3NH_3PbX_3(s) \rightarrow PbX_2(s) + CH_3NH_2(g) + HX(g) \quad \text{(P1)}$$

$$CH_3NH_3PbX_3(s) \rightarrow PbX_2(s) + CH_3X(g) + NH_3(g) \quad \text{(P2)}$$

The decomposition pathway of $MAPbX_3$ is still under debate because the decomposition products from both pathways have been experimentally measured.[53,54] A recent study on thermal decomposition of $MAPbI_3$ showed that both of the decomposition pathways are possible and also depend on temperature.[55] Pathway (P2), which is thermodynamically favored over pathway (P1), becomes favorable as temperature increases because kinetic hindrance of pathway (P2) is mitigated at high temperatures.[55]

Thermogravimetric analysis measures weight loss of MHPs as temperature is increased; the onset of weight loss indicates volatilization of breakdown products, and is therefore a measure of the stability of the compound.[56–58] MABr begins to decompose at 200 °C,[56] and $MAPbX_3$ begins to decompose at 200–300 °C (≈220 °C for $MAPbBr_3$,[56] ≈200 °C,[58] ≈250 °C,[57] and ≈294 °C[53] for $MAPbI_3$). The decomposition onset temperature of 200–300 °C may be regarded as thermally stable, but many researchers have reported that thermal degradation can occur at temperatures <200 °C.[59–63] The optimal annealing temperature to give the best PCE of $MAPbI_3$ PeSCs is ≈100 °C; further increase in this temperature degrades device efficiency by damaging the MHP layers, as proven by the occurrence of PbI_2 peaks at temperatures >120 °C in the X-ray diffraction (XRD) patterns.[59] Also, the intensity of PbI_2 peak in XRD patterns of $MAPbI_3$ films is significantly increased by thermal annealing at 140 °C for 30 min, whereas the increase is negligible at 100 °C.[60] The thermal degradation of $MAPbI_3$ layers can be clearly visualized by conductive atomic force microscopy (c-AFM) measurement (**Figure 2**).[61] Even in a nitrogen atmosphere, the annealing of $MAPbI_3$ layers at 85 °C for 24 h was shown to cause a significant amount of current-less dark area as a result of the degradation of the $MAPbI_3$.[61] These experiments clearly show that $MAPbI_3$ is not thermally stable.

$MAPbBr_3$ has a stable cubic crystal structure and higher Pb—X bond strength than $MAPbI_3$, and therefore has relatively better thermal stability than $MAPbI_3$.[43,63] Irradiation of 100 suns on $MAPbI_3$ films at elevated temperature of 45–55 °C reduces its absorption, but $MAPbBr_3$ films were found to be stable under the same conditions.[63] However, $MAPbBr_3$ also experiences slight thermal degradation even at <100 °C. Increasing the annealing time of $MAPbBr_3$ emission layers from 10 to 30 min (at 90 °C) causes slight sublimation of MABr and reduces crystallinity, and thereby decreases the EL efficiency of $MAPbBr_3$ PeLEDs.[62]

The thermal instability of $MAPbI_3$ and $MAPbBr_3$ can be understood by calculating the enthalpy of formation from MAI (or MABr) and PbI_2 (or $PbBr_2$).[64,65] The calculated enthalpies of formation were 34.50 kJ mol^{-1} for $MAPbI_3$ and 6.69 kJ mol^{-1} for $MAPbBr_3$.[64] These positive enthalpies of formation indicate that $MAPbI_3$ and $MAPbBr_3$ are thermodynamically unstable. A density functional theory (DFT) calculation also yielded the formation enthalpies of $MAPbI_3$ (–0.1 eV = –9.65 kJ mol^{-1}), $MAPbBr_3$ (–0.25 eV = –24.12 kJ mol^{-1}), and $MAPbCl_3$ (–0.7 eV = –67.54 kJ mol^{-1}); the comparison indicates that $MAPbI_3$ is more thermodynamically unstable than $MAPbBr_3$ and $MAPbCl_3$.[65] However, contradictory to the results mentioned above, a study on thermal and thermodynamic stability of $MAPbX_3$ (based on nonambient XRD and Knudsen effusion mass spectrometry) concluded that $MAPbCl_3$ is more thermally and thermodynamically unstable than $MAPbBr_3$ and $MAPbI_3$, and that $MAPbI_3$ is kinetically more stable than $MAPbBr_3$, although $MAPbI_3$ has smaller negative enthalpy of formation than $MAPbBr_3$ (–403.6 ± 9.7 kJ mol^{-1} for $MAPbI_3$ and –567.5 ± 8.7 kJ mol^{-1} for $MAPbBr_3$).[54]

2.1.3. Influence of Atmosphere on Stability

Atmospheric gases (oxygen and water) have profound influence during fabrication and during device operation. MHPs are considered chemically inert in nitrogen (and in other inert gases) and in vacuum. In the presence of residual humidity, water diffuses quickly in MHPs (time-scale of seconds) and the process occurs readily at relatively low levels of humidity (RH ≈ 10%).[66] In PeSCs, moderate levels of humidity causes water-assisted resolvation and recrystallization of MHPs, and therefore is widely considered to be beneficial during device fabrication.[67–70] However, humidity can accelerate the degradation of MHPs under illumination. Ab initio molecular dynamics simulations have further revealed surface reconstruction and light-assisted formation of hydrated species of $MAPbI_3 \cdot H_2O$; these phenomena explain why simultaneous exposure to water and light accelerates degradation of MHPs.[71,72] Despite the fast diffusion of water within MHP layers, PeLEDs based on a $CsPbBr_3$–polymer composite retain basic operation ability when operated under ambient conditions (RH ≈ 60% and 30 °C);[73] this temporary stability indicates that cladding the MHPs with organic (polymer and organic small molecules) or inorganic layers provides at least some barrier function against diffusion of atmospheric components.[74,75]

The influence of oxygen is more complex than that of other gases. Some reports link the presence of oxygen

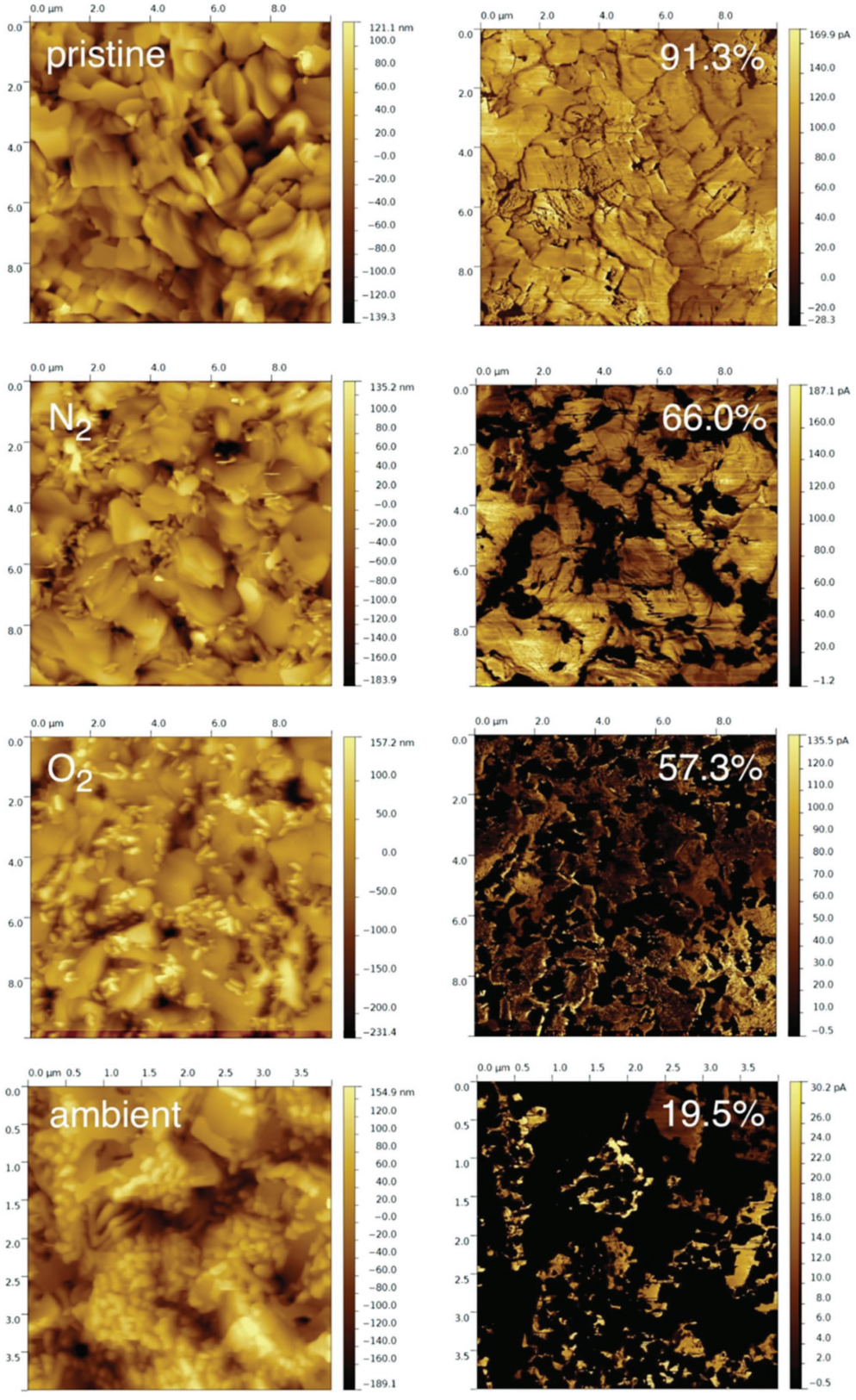

Figure 2. Atomic force microscopy topography (left column) and current mapping (right column) images of $MAPbI_3$ films that were subjected to 85 °C for 24 h at different atmospheres. The percentages in the right column indicate the fraction of bright area that contributes to the measured current. Reproduced with permission.[61] Copyright 2015, Wiley-VCH.

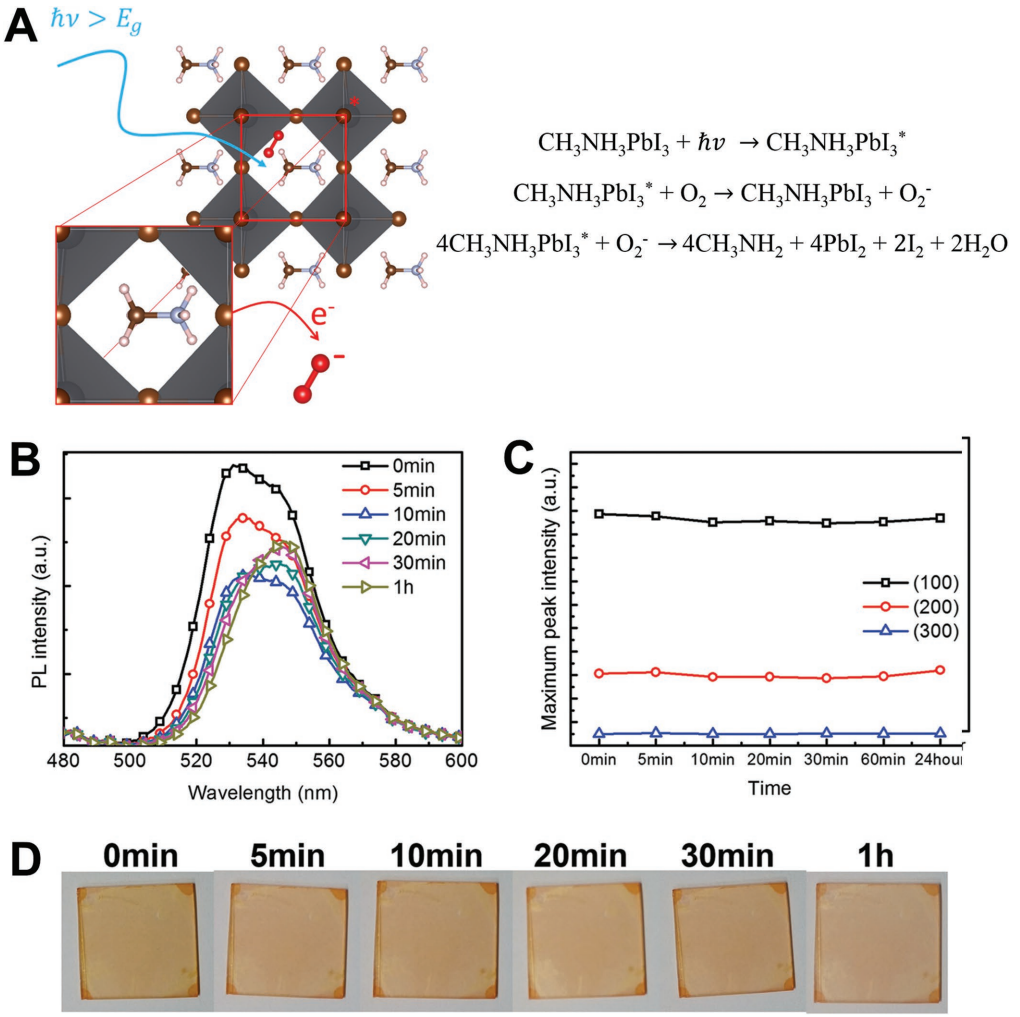

Figure 3. A) Graphical representation of the degradation mechanism of $MAPbI_3$ in the presence of light and oxygen. Absorption of a photon leaves $MAPbI_3$ in an excited state $MAPbI_3$*. Transfer of the photoexcited electron from $MAPbI_3$* to O_2 generates superoxide O_2^-. Superoxide decomposes the MHP with generation of methylamine (CH_3NH_2), the lead salt PbI_2, iodine, and water.[76] The crystal structure was visualized using VESTA.[77] B–D) PL spectra (B), maximum XRD peak intensities (C), and photographs (D) of $MAPbBr_3$ films with increasing air-exposure time. Reproduced with permission.[15] Copyright 2014, Wiley-VCH.

(and photoexcitation) to an increase of luminescence properties, ("oxygen-boost"),[78] whereas others have linked the presence of oxygen to degradation.[79,80] The boost effect has been demonstrated by atmosphere-dependent PL experiments; its origin has been identified as light-induced trap states that are efficiently passivated by oxygen.[81] This phenomenon is closely related to the passivation of defects by Lewis bases,[82,83] which are thought to passivate the dangling bonds of Pb left behind by formation of halide vacancies.[84] The oxygen-related degradation mechanism was proposed to be based on the formation of superoxide species (O_2^-) in the presence of ultraviolet (UV) light and oxygen (**Figure 3**A).[76,79] Its reaction with the MA moiety leads to rapid decomposition of the perovskite, and replacing MA^+ with an unprotonated cation may therefore lead to an MHP with increased stability with respect to oxygen and light.[76] The validity of this idea is supported by the increased humidity and photostability of $CsPbBr_3$ over organic–inorganic hybrid perovskites in some cases,[56,85] but the thermal stability of $CsPbBr_3$ is also higher, so the effects are difficult to discern. Degradation mechanisms include redox reactions at electrodes or interlayers (Section 2.2).[74,86] However, $MAPbBr_3$ films have also showed moderate air stability in the absence of high-power illumination:[15] during air exposure of 1 h, the PL intensity of $MAPbBr_3$ films just slightly decreased until 10 min and was then saturated, and their XRD patterns and color did not even change (Figure 3B–D).

2.1.4. Influence of Light Exposure on Stability

Exposure to light degrades MHPs even in the absence of additional degradation pathways such as light-induced generation of superoxide O_2^-.[87,88] Femtosecond pump-probe spectroscopy indicates that MABr and MAI readily dissociate under a 266 nm pump; this result implies that UV exposure inevitably accelerates degradation of organic–inorganic hybrid perovskites.[89] In $MAPbI_3$, the degradation is further supplemented by photodissociation of I_2 into 2I, and by subsequent decomposition of

$MAPbI_3$, as indicated by accelerated degradation of $MAPbI_3$ films after exposure to I_2 vapor.[53,90] This reaction suggests that the mechanism associated with the photodissociation of halide species might be suppressed by using Ruddlesden–Popper (RP) layered MHP materials instead of 3D MHPs; in fact, PeSCs with 3D/2D MHP interfaces have considerably increased operation lifetimes (10 000 h at PCE ≈ 11%).[91] MHP films are usually considered stable under pulsed laser excitation[92–94] but because of the low bond strength,[95] low Debye temperature (≈300 K for $MAPbBr_3$),[13] and the resulting high ion mobility (Section 2.2.1), the films may not be stable under continuous-wave excitation.[96]

2.1.5. Instability of MHP NPs in Solution and Film States

MHP NPs have shown very high PLQE (≈90%) in the solution state, and can be produced by a variety of synthesis and film-formation processes.[2,6,30,40,97,98] After the first EL from MHP NPs was reported,[99,100] EL efficiencies dramatically increased to ≈13.3 cd A^{-1} for green emission and to ≈3.4 cd A^{-1} for red emission;[101,102] however, the operational stability of PeLEDs based on MHP NPs is rarely reported. We considered and categorized the reasons of these few reports: (i) intrinsically unstable perovskite crystal structure in solution and film states due to unstable organic A-site cations and colloidal instability;[98,103–108] (ii) excessive removal or inappropriate treatment of surface ligands on NPs;[101,109] and (iii) inhomogeneous morphology of NP films with pinholes due to easily aggregated or agglomerated NPs in film and solution states; these pinholes reduce the EL efficiency of PeLEDs.[101,102,106,110,111]

The PLQE of $MAPbBr_3$ NPs is easily degraded in the solution state, possibly because MA^+ cations have low chemical stability in the presence of moisture and heat.[98,106] Although $CsPbBr_3$ NPs in solutions[98,106] and bulk polycrystalline films[112] have shown much improved stability compared to those of $MAPbBr_3$ NPs and films, the PLQE of $CsPbBr_3$ NPs dramatically reduced (<10%) when they were formed into film states.[105] Organic ligands on the surface of MHP NPs are necessary for stabilizing and processing NPs in the solution and film states, but the insulating alkyl chains in the ligands prevent efficient charge injection/transport in the film state, and thereby reduce device efficiency. Thus, ligand engineering to replace the long alkyl chains with short chains, or to eliminate the ligands on MHP NPs, should be conducted to further increase the EL efficiency. However, incomplete ligand exchange or excessive elimination of surface ligands induces aggregation or agglomeration (e.g., from 8.1 nm sized NPs to 20 nm) and thus dramatically reduces the stability and PLQE of MHP NPs.[101,109] The low PLQE and stability of MHP NP films can reduce the EL efficiency and the operational stability in LED devices. MHP NPs in the solution state also showed low colloidal stability when at a concentration of >5 mg mL^{-1},[110] and they can also easily aggregate or agglomerate during film formation; the result is a rough film morphology (root-mean-square roughness of ≈45.3 nm).[111] These tendencies cause pinholes that prevent the formation of uniform NP films and thus reduce the operational stability of PeLEDs by inducing a leakage current.[110,111] To achieve high-stability NP-based PeLEDs, these low stabilities of MHP NPs in solution and film states must be solved.

2.2. Instability in PeLED Devices

In general, PeLEDs consist of MHP emission layers, charge-injection/transport layers, and electrodes (anode and cathode). Apart from the instability of the MHP emission layers, additional instabilities of PeLEDs originate from the other layers, interfaces, and the electrical stress during operation of PeLEDs. The main cause of the instability in PeLEDs is electric-field-induced ion migration that can destroy MHP lattices, generate defects,[113] corrode electrodes,[39,114,115] degrade charge-transport layers,[116] and form charge-accumulated interfaces[117] and a p–i–n junction.[73,118–120] Furthermore, diffusion of metallic species from electrodes can cause a significant decrease in EL efficiency and accelerate the degradation of PeLEDs.

2.2.1. Ion-Migration-Induced Degradation

Because of the complex ABX_3 stoichiometry, MHP ionic crystals host a variety of defects. These include Schottky defects (cation and anion vacancies), Frenkel defects (interstitial sites), antisite defects, and structural defects (grain boundaries, interfaces, and lattice distortion by impurities).[113] The soft lattices of MHP materials with small defect-formation energy (e.g., 27–73 meV for PbI_2 vacancies[84]) allow constituent ions to escape easily from the lattices and to move along these defect sites.[113] Especially, the grain-boundary area is a main channel for ion migration.[121]

The mobility μ_m[cm^2 V^{-1} s^{-1}] of ion migration can be expressed as[122]

$$\mu_m = \frac{A}{T}\exp\left(\frac{-E_{a,m}}{k_B T}\right) \tag{3}$$

where $E_{a,m}$ [eV] is the activation energy for ion migration, $k_B = 8.617 \times 10^{-5}$ eV K^{-1} is the Boltzmann constant, A is a material-dependent constant, and T[K] is the absolute temperature. $E_{a,m}$ is a measure of how easily ions can migrate; it depends on many characteristics of the crystal structure, such as the radius of the ions, the jumping distance between adjacent defects, and the charge of the ions.[113] Recent theoretical and experimental studies have revealed that the migration of halide anions is predominant over the migration of A-site cations and lead cations, because halide anion migration has the smallest $E_{a,m}$ (0.09 eV in $MAPbBr_3$,[123] 0.08–0.58 eV in $MAPbI_3$,[123–125] and 0.09[7] and 0.25 eV[126] in $CsPbBr_3$). Measurements of ionic conductivity indicates that Br^- migration in $CsPbBr_3$ has $E_{a,m}$ = 0.25 eV.[126] Temperature-dependent analysis of $CsPbBr_3$ PeLEDs showed that the current-hysteresis area increases exponentially as T increases, with an activation energy of 90 ± 7 meV, and that the current hysteresis is mainly caused by Br^- ion migration.[7] The halide anion migration occurs through vacancies of halide anions, not through interstitial sites;[127] this was proven by a decrease in the ionic conductivity on increasing the iodine partial pressure, obtained by a direct-current (DC) galvanostatic polarization method.

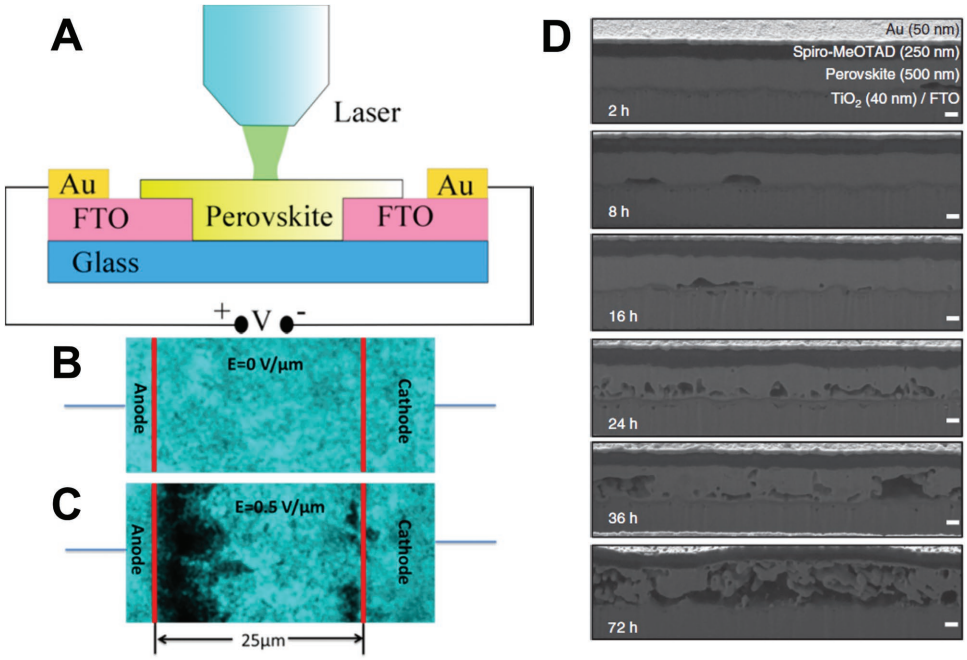

Figure 4. A) Schematic sample structure (a lateral device, Au/fluorine doped tin oxide (FTO)/$MAPbBr_3$/Au). B,C) Optical images of the sample with an electric field (B), and without an electric field (C). D) Time evolution of cross-section of a PeSC device for 72 h under illumination in ambient conditions (scale bar = 200 nm). A–C) Reproduced with permission.[128] Copyright 2016, American Chemical Society. D) Reproduced with permission.[117] Copyright 2016, Nature Publishing Group.

The ion migration is one of the main origins of degradation in PeLEDs. Electrical stress on MHP layers can facilitate migration of ions, which can accumulate at defect sites or at interfaces with other layers, and cause significant degradation of the MHP layers.[117,128] Optical imaging of a lateral structure of anode/$MAPbBr_3$/cathode under continuous illumination with and without applied electric field (0.5 V μm^{-1}) has shown that a dark region is formed at the anode side only when an electric field is applied (**Figure 4**A–C).[128] The illuminated $MAPbBr_3$ layers exhibited an excitation-density-dependent decrease in PL intensity and lifetime; these results demonstrate that Br^- anion migration is activated under high excitation density and induces nonradiative recombination, which decreases PL intensity and lifetime.[128] Therefore, ion migration in MHPs can also contribute to EL quenching and the low operational stability of PeLEDs. Light soaking generates trapped charges at grain boundaries and interfaces; the trapped charges can trigger irreversible degradation of MHP layers in the presence of moisture (Figure 4D).[117] These results imply that the degradation of MHP layers can be facilitated under applied bias that induces ion migration and consequently increases the accumulation of charges at the interfaces.

Also, ion migration from MHP layers can lead to corrosion of metal electrodes. The electric-field-induced ion migration can cause accumulation of ions at interfaces with metal electrodes; the accumulated ions can corrode the electrodes.[39,114,115,129] Migration of I^- anions corrodes metal electrodes (e.g., Ag, Al) and creates insulating components (e.g., AgI).[114,115,129] The presence of AgI was indicated by a peak at 619.4 eV that can be assigned as Ag—I bonds in the I 3d spectrum of X-ray photoelectron spectroscopy,[114] and by a color change,[39,115] and by scanning electron microscopy with energy-dispersive X-ray analysis.[129] The insulating AgI components facilitate degradation of PeSCs[114,115] and PeLEDs,[39] possibly by generating deep traps[114] or by blocking efficient charge injection and extraction.

Another study on the degradation of PeLEDs concluded that spontaneous redox reactions between metal electrodes and Pb^{2+} cations in MHPs cause oxidation of the metal electrodes and decomposition of the MHP layers.[86] The redox reactions occurred only when $MAPbI_3$ or PbI_2 layers, which contains Pb^{2+} cations, were in contact with metal electrodes (e.g., Al, Ag, Cr, and Yb); these reactions were accelerated by moisture. The suggested pathway for redox reaction between Al and $MAPbI_3$ was[86]

$$2Al + 4CH_3NH_3PbI_3 + 2H_2O \rightarrow (CH_3NH_3)_4 PbI_6 \cdot 2H_2O + 3Pb + 2Al^{3+} + 6I^- \quad (P3)$$

$$2Al + 3(CH_3NH_3)_4 PbI_6 \cdot 2H_2O \rightarrow 12CH_3NH_3I + 3Pb + 2Al^{3+} + 6I^- \quad (P4)$$

However, these reaction pathways do not provide a full understanding of why halide anion migration facilitates the corrosion of metal electrodes. Therefore, pathways for the corrosion of metal electrodes facilitated by accumulation of halide anions need to be further investigated.

Furthermore, ion migration can cause degradation of the hole-transport layers, including 2,2′,7,7′-tetrakis(*N*,*N*-di-p-methoxyphenylamine)-9,9′-spirobifluorene (spiro-MeOTAD) by forming spiro-MeOTAD–I coordinations, and consequently reduce the hole-transporting ability;[116] this result suggests that

other materials that are used as hole-transport layers in PeLEDs can also be degraded by coordination with migrated halide anions.

Although electrical-field-induced ion migration degrades device stability in the long run, it does not always hamper EL in PeLEDs. Electrical stress on PeLEDs temporarily increases luminance and EL efficiency, possibly due to trap filling.[7,34,51,52,73,130,131] For example, the luminance of a $CsPbBr_3$ PeLED increased by >300% at 350 s of operation, then decreased.[7] Under multiple electrical scans of PeLEDs at different temperatures (180, 220, 260, 300 K), luminance and EQE increased with the number of scans only at 260 and 300 K; the authors ascribed the temporal increase in luminance and EL efficiency to trap filling by local migration of excess mobile ions, and ascribed the maintenance of the luminance and EL efficiency at lower temperatures (180 and 220 K) to reduced coupling between the trap-assisted nonradiative recombination and phonon modes as temperature is decreased.[52] Also, the decrease in the EQE by long-term electrical stress was ascribed to migration of nonexcess ions in the perovskite lattice, and consequent generation of defects.[52] The improvement in the interface contact, and the effect of film annealing by Joule heating were also suggested as origins of luminance enhancement by electrical stress.[112] In addition, the luminance enhancement by electrical stress may be due to improved charge injection into MHP layers by narrowing the injection-barrier width as a result of electric-field-driven ion migration and accumulated charge at the interfaces; similar behavior has been reported in conventional light-emitting electrochemical cells (LECs).[132–138] These propositions for temporal luminance improvement by electrical stress must be further explored.

2.2.2. The Formation of a p–i–n Junction

MHP materials are not purely electronic conductors (Section 2.2.1); they should be considered as both electronic and ionic conductors. For this reason, some researchers have considered PeLEDs as MHP LECs (PeLECs) where light emission occurs in the intrinsic region of a p–i–n junction.[100,139] Such junctions may form in single-layer PeLEDs (anode/MHP emission layer/cathode structure) during their operation;[73,118–120] this mechanism is similar to that of conventional LECs, in which emission layers are generally composed of light-emitting conjugated polymers mixed with ionic conductors.[132–138] Ion migration in MHP layers under an external electrical field can cause accumulation of ions near the electrode sides, and thereby lead to p- and n-doping starting from the electrodes; the p- and n-doping frontiers propagate toward each other and consequently form a reversible p–i–n homojunction structure.[140] The hypothesis that a p–i–n junction forms was also supported by quantification of ionic conductivity and the luminance–voltage characteristics of PeLEDs based on MHP–polymer composites.[118] Poly(ethylene oxide) (PEO) was used as an ionic-conducting polymer, and poly(vinylidene fluoride) (PVDF) was used as a polymer with poor ionic conductivity. The MHP–PEO PeLEDs had ≈50 000 times higher ionic conductivity and one-quarter the turn-on voltage of those of MHP–PVDF PeLEDs; these results support the hypothesis that the operational mechanism of PeLEDs is related to the p–i–n junction.[118] This hypothesis about the formation of a p–i–n junction was also verified by time-dependent discharging current measurement,[73,119] photocurrent response,[73] alternating-current impedance spectroscopy,[119] turn-on voltage independent on MHP layer thickness,[119] and postbias photocurrent mapping.[120]

In the short term, the formation of a p–i–n junction can facilitate charge injection by evolving a sharp tunneling barrier that lowers the effective charge-injection barrier.[73] However, over time, the formation of a p–i–n junction can decrease the stability of PeLEDs. In conventional LECs, the major stability-limiting processes are the irreversible electrochemical degradation of light-emitting polymers at the light-emitting p–n junction line,[137] the nonuniformity of p- and n-doped frontiers that causes a short circuit when the frontiers contact to electrodes,[133] and phase separation between the ionic materials and the light-emitting polymers.[132] However, PeLEDs usually have single-component MHP emission layers, so phase separation can be excluded. Also, the nonuniformity of doping frontiers may not be a main degradation mechanism in PeLEDs because the dynamic junction in MHP layers was very broad, like a recombination zone in OLEDs,[119] whereas the dynamic junction has the form of a wavy line in conventional LECs.[132–138] However, although the electrochemical degradation mechanism of light-emitting polymers is totally different from that of MHPs, electrochemical degradation of MHPs in the recombination zone may be possible and should be further investigated.

The operational lifetime of PeLEDs is significantly increased at liquid-nitrogen temperature (−193 °C) at which the motion of ions is restricted, compared to the lifetime at room temperature.[119] This result suggests that degradation of PeLEDs may be ascribed to the disappearance of an intrinsic region and the protrusion of p- and n-doped regions in the opposite directions as a result of p–i–n junction propagation, as in conventional LECs.[119] In addition, other reasons such as the prevention of trapped-charge-induced degradation[117] and reduced trap-assisted nonradiative recombination[52] should be considered for lifetime improvement (Section 2.2.1).

2.2.3. Diffusion of Metallic Species from Electrodes

One of the important causes of the degradation of MHP layers in PeLEDs is diffusion of metallic species from electrodes. To investigate the diffusion of metallic species, the depth profile of the constituent elements throughout an entire MHP solar-cell device (FTO/TiO_2/mesoporous TiO_2/MHP/spiro-MeOTAD/gold) was conducted using time-of-flight secondary-ion mass spectroscopy (TOF-SIMS).[141] A Au^- anion signal was detected at the TiO_2 layer of the device annealed at 70 °C for >15 h under 1 sun illumination. Metallic species in the middle of devices can provide shunting paths and create deep-trap states or luminescence quenching centers that increase nonradiative recombination, so the accumulation of metallic species in the MHP layers and charge-transport layers can be critical for both the PCE of PeSCs and the EL efficiency of PeLEDs (**Figure 5**A).[1,141] Therefore, prevention of diffusion of metallic species has been an important issue in the OLED field.

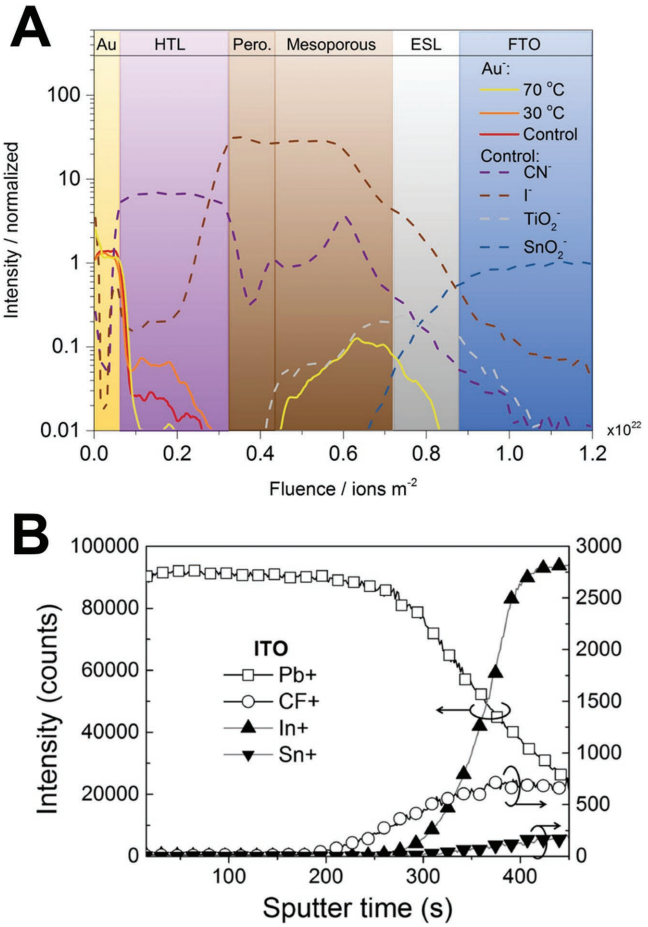

Figure 5. A,B) TOF-SIMS depth profiles of PeSC devices (aged at 30 and 70 °C) with structure of FTO/TiO_2/mesoporous TiO_2/MHP/spiro-MeOTAD/gold (A) and ITO/Buf-HIL/$MAPbBr_3$ films (B). A) Reproduced with permission.[141] Copyright 2016, American Chemical Society. B) Reproduced with permission.[37] Copyright 2017, Wiley-VCH.

Diffusion of In and Sn atoms from indium tin oxide (ITO) electrodes can also cause degradation. When acidic poly (3,4-ethylenedioxythiophene):polystyrene sulfonate (PEDOT:PSS) is used as the hole-injection layer for PeLEDs, the PEDOT:PSS can etch the underlying ITO electrodes and thereby cause release of In and Sn atoms.[22,37] The released In and Sn atoms can diffuse into the PEDOT:PSS and MHP layers and accelerate the degradation of the PeLEDs (Figure 5B) because the metallic species can be luminescence-quenching centers.[37] In PeLEDs in which the electron–hole diffusion lengths are very long (>1 µm),[142] luminescence quenching by impurity and migrated metal species can be more critical compared with OLEDs in which the exciton diffusion lengths are short (5–10 nm).[143] Therefore, prevention of diffusion of metallic species toward emission layers will be a very important task to improve the device efficiency and lifetime.

2.2.4. Color Instability

One of the important challenges to realize high-stability PeLEDs is to stabilize the emission color. Because the color of PeLEDs mainly depends on the halide anions, halide separation in mixed-halide MHP emission layers can cause a change in emission color.[139,144,145] Halide separation is a result of the phase instability of mixed-halide MHPs.[146,147] A DFT calculation on the phase diagram of $MAPb(I_{1-x}Br_x)_3$ solid solutions revealed that they have a miscibility gap at room temperature, binodal points at $x = 0.2$ and 0.7, and undergo spinodal decomposition at $0.3 < x < 0.6$.[146] The phase instability of mixed-halide MHP systems ($MAPb(I_{1-x}Br_x)_3$) was clearly visualized by cathodoluminescence imaging, which showed the emergence of I-rich clusters and the increase in the number of clusters with increasing light-soaking time (**Figure 6**).[147] The halide separation in $MAPb(I_{1-x}Br_x)_3$ was also well explained by a molecular dynamics simulation; the result suggested that localized lattice strain induced by coupling between photogenerated charges and phonon modes drives phase separation.[147]

Halide separation was shown in the driving-voltage-dependent EL spectrum of $MAPbBr_{3-x}I_x$ PeLECs.[139] As the voltage was increased from 2.0 to 7.0 V, the EL spectrum gradually shifted from 743 to 710 nm, and a green EL peak at 532 nm emerged beginning at 6.0 V.[139] Because the green EL peak corresponds to the emission of $MAPbBr_3$, the change in the EL spectrum was explained by the migration of I^- anions.[139] Also, an electrical field can drive halide separation in $CsPbBr_{1-x}I_x$ NP PeLEDs.[144] The PeLEDs that incorporated $CsPbBr_{1.88}I_{1.12}$ NPs that emitted orange PL at 558 nm, instead emitted red EL at 650 nm after turn-on; the EL emission was split into a green emission at 518 nm (i.e., the emission of $CsPbBr_3$) and a red emission at 665 nm (i.e., the emission of $CsPbBr_{0.5}I_{2.5}$);[144] over time, the intensity of the green emission increased, whereas the intensity of the red emission decreased and eventually disappeared. This color instability is a result of the production of pure $CsPbBr_3$ domains by ion migration induced by an electrical field, without red-emitting neighboring domains that could induce Förster resonance energy transfer.[144] After the PeLEDs were turned off, orange and green PL emissions were both observed; this result means that halide separation is partially reversible and that in the absence of an electric field, halide anions redistribute among NPs.[144]

3. Strategies to Improve the Stability of MHP Materials and PeLEDs

In this section, we review recently reported strategies to overcome the instability of MHP materials and the limited operational stability of PeLEDs (**Figures 7** and **8**). Recently, the operational stability of PeLEDs has been significantly improved, but it is still much inferior to the stability of OLEDs (L_{50} > 500 000 h at 1000 cd m^{-2})[148] and QD LEDs ($L_{50} \approx$ 300 000 h at 100 cd m^{-2}).[26] We have conducted an exhaustive survey on the reported operational lifetime of PeLEDs (**Table 1**). The operational lifetimes of PeLEDs can be characterized by the time taken for the luminance to decay from the initial luminance L_0 to 50%, 70%, and 80% (defined as L_{50}, L_{70}, and L_{80}, respectively). However, the summarized studies have different measurement conditions for operational lifetime. To effectively compare the operational lifetime among the reported devices, the measurement conditions should be standardized as in the field of OLEDs; the initial luminance should be reported (commonly used initial

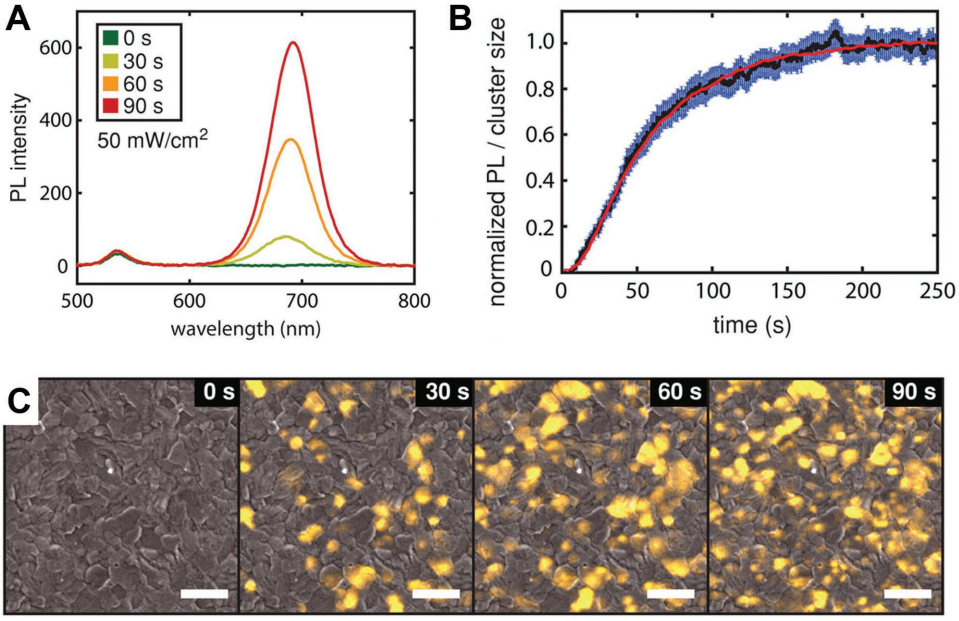

Figure 6. A) PL spectra of a $MAPb(I_{0.1}Br_{0.9})_3$ film after different light exposure times (0, 30, 60, 90 s). B) Normalized PL intensity (red) and normalized cluster size (black) with standard error (blue) versus light exposure time. C) Cathodoluminescence image series with light exposure of 30 s between each image (scale bar = 2 µm). Reproduced with permission.[147] Copyright 2017, American Chemical Society.

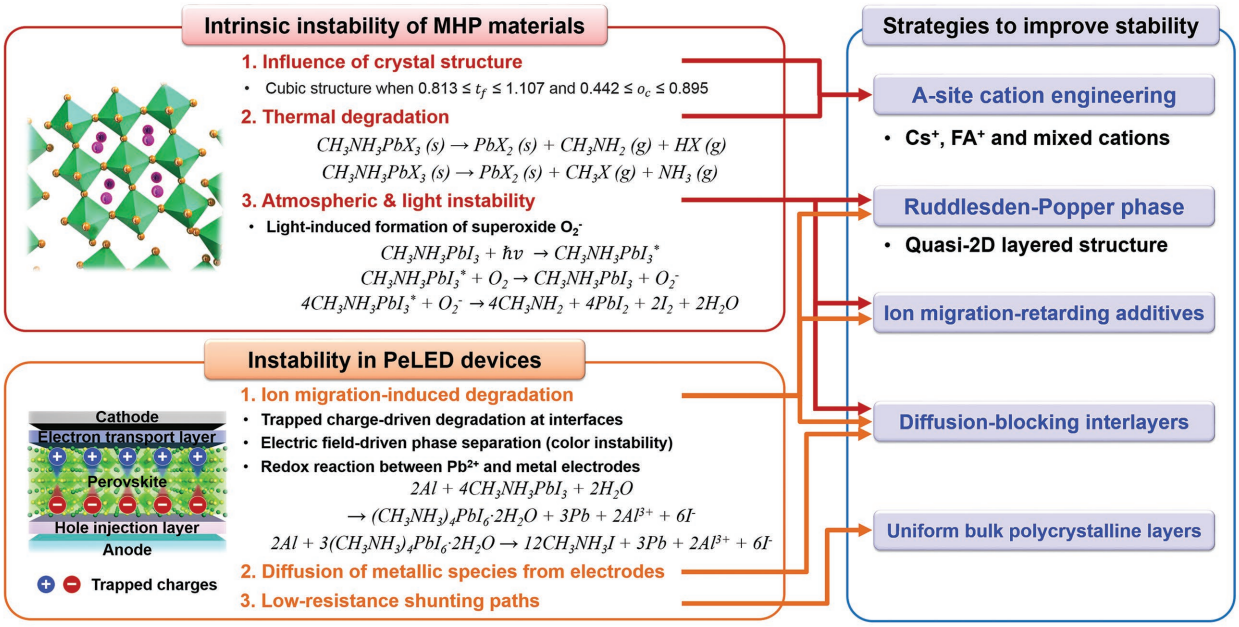

Figure 7. Schematic diagram that summarizes representative instability of MHP materials and PeLED devices with chemical reactions[43,53–55,76,86] and corresponding solutions.

luminance: 100 and 1000 cd m^{-2}) and the operation of PeLEDs should be continuous at a constant current or voltage without any interval. To date, the longest reported lifetime of PeLEDs is $L_{50} \approx 10$ d (from PeLEDs based on $MAPbBr_3$ NPs).[110] However, the origin of the lifetime enhancement and measurement conditions was not reported. Also, PeLEDs based on $CsPbBr_3$–PEO composites showed an operational lifetime of $L_{80} \approx 80$ h,[149] but mechanism for the lifetime enhancement should be further studied.

3.1. A-Site Cation Engineering

A simple method to improve the stability of MHPs is the use of A-site cations (e.g., FA^+ and Cs^+), which are more stable than MA^+ cations. The use of large organic ammonium (OA) cations can also improve the stability of MHPs by forming an RP phase, but this approach will be discussed in Section 3.2. The use of FA-based MHPs ($FAPbX_3$) can increase the

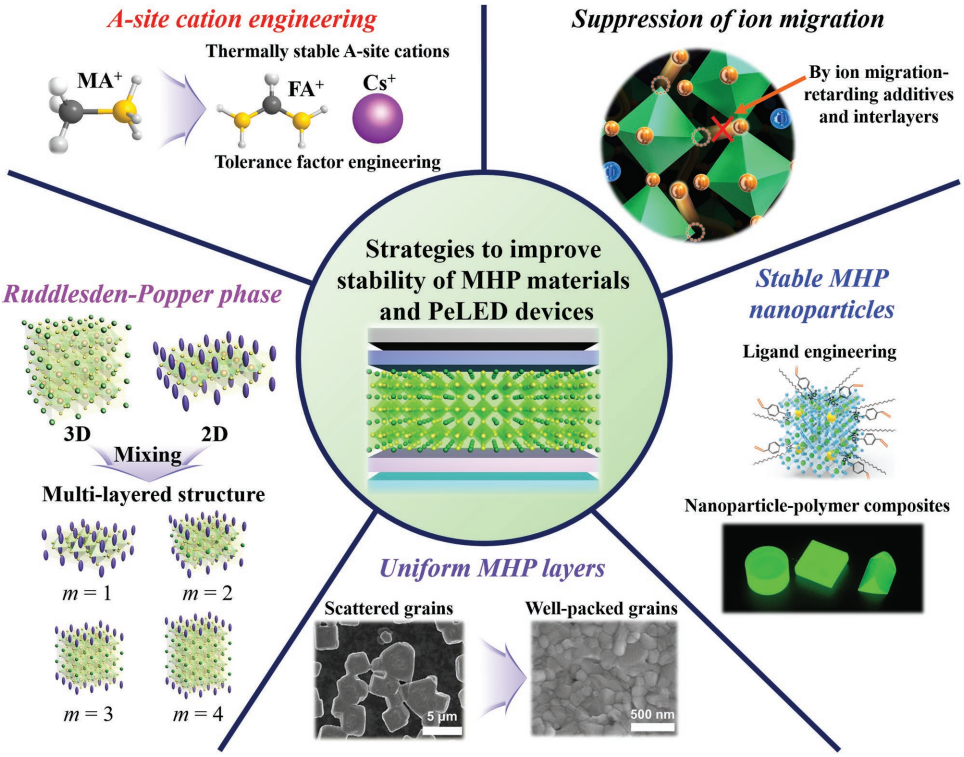

Figure 8. Schematic illustration describing the strategies to improve the stability of MHP materials and PeLEDs. Figures in the section of the RP phase are reproduced with permission.[33] Copyright 2016, Wiley-VCH. Figures in the section of uniform MHP layers are reproduced with permission.[1] Copyright 2015, The American Association for the Advancement of Science. Figures in the section of stable MHP nanoparticles are reproduced with permission.[150] Copyright 2017, Wiley-VCH.

Table 1. The reported operational lifetime of PeLEDs.

Refs.	Publication year/month	Device structure	Emission layer	Operational lifetime	Lifetime measurement conditions
Song and co-workers[151]	2015/05	ITO/TiO_2/EA/MHP/SPB-02T/MoO_3/Au	$MAPbBr_3$	$L_{50} \approx 55$ h	$L_0 \approx 120$ cd m^{-2}, at 4.8 V
Mathews and co-workers[152]	2015/10	ITO/PEDOT:PSS/MHP/F8/Ca/Al	$CsPbBr_3$	$L_{50} \approx 9.5$ min	At 7 V
Choy and co-workers[153]	2016/01	ITO/PEDOT:PSS/poly[*N*,*N*′-bis(4-butylphenyl)-*N*,*N*′-bis(phenyl)-benzidine] (poly-TPD)/PFI/MHP/1,3,5-tris(*N*-phenyl-benzimidazol-2-yl)benzene (TPBI)/LiF/Al	$CsPbBr_3$ NPs	$L_{50} \approx 10$ min	At 5 V
Zhang and co-workers[110]	2016/05	ITO/PEDOT:PSS/poly(9-vinylcarbazole) (PVK)/MHP/TPBI/LiF/Al	$MAPbBr_3$ NPs	$L_{50} \approx 10$ d	Not reported
Song and co-workers[154]	2016/05	ITO/PEDOT:PSS/MHP/SPW-111/LiF/Ag	$MAPbBr_3$	$L = L_0$ for >162 cycles	$L_0 \approx 1180$ cd m^{-2}, at 3.8 V, noncontinuous test
Wei et al.[112]	2016/09	ITO/PEDOT:PSS/MHP/4,6-*bis*(3,5-di(pyridin-3-yl)phenyl)-2-methylpyrimidine (B3PYMPM)/$CsCO_3$/Al	$CsPbBr_3$:CsBr = 1:0.4 (molar ratio)	$L > L_0$ for >15 h	$L_0 \approx 100$ cd m^{-2}, at 66.67 mA cm^{-2}
Yu and co-workers[73]	2016/09	ITO/MHP/In:Ga	$CsPbBr_3$:PEO:polyvinylpyrrolidone (PVP) = 100:50:5 (weight ratio)	$L > L_0$ for >1 h	$L_0 \approx 100$ cd m^{-2}, at 2.7 V
Lam and co-workers[155]	2016/09	ITO/PEDOT:PSS/poly-TPD/MHP/TPBI/Al	$BA_2MA_2Pb_3I_{10}$	$L_{50} \approx 85$ s	At 4 V
Huang and co-workers[5]	2016/09	ITO/ZnO/PEIE/MHP/poly[(9,9-dioctylfluorenyl-2,7-diyl)-co-(4,4′-(*N*-(4-sec-butylphenyl)diphenylamine)] (TFB)/MoO_x/Au	NMAI: formamidinium iodide (FAI):PbI_2 = 2:1:2 (molar ratio)	$L_{50} \approx 100$ min	At 10 mA cm^{-2}
Zhang and co-workers[156]	2016/12	Au/p-MgNiO/MHP/poly(methyl methacrylate) (PMMA)/n-MgZnO/n^+-GaN	$CsPbBr_3$ NPs	$L_{80} \approx 9$ h	At 10 V, unencapsulated, under ambient condition (RH = 30–50%)

Table 1. Continued.

Refs.	Publication year/month	Device structure	Emission layer	Operational lifetime	Lifetime measurement conditions
Song and co-workers[31]	2017/01	ITO/PEDOT:PSS/MHP/TPBI/LiF/Ag	$MAPbBr_3$	$L_{50} \approx 55$ min	At 50 mA cm^{-2}
Rand and co-workers[4]	2017/01	ITO/poly-TPD or PVK/ MHP/TPBI/LiF/Al	n-butylammonium iodide (BAI):$MAPbI_3$ = 20:100 (near infrared (NIR)) BABr:$MAPbBr_3$ = 20:100 (green)	$L_{70} \approx 300$ min (NIR) $L_{50} \approx 48$ min (green)	At 3 mA cm^{-2}
bin Mohd Yusoff and co-workers[157]	2017/02	ITO/ZnO NPs/MHP/ *N*,*N*′-bis(1-naphthyl)-*N*,*N*′-diphenyl-1,1′-biphenyl-4,4′-diamine (α-NPD)/MoO_3/Al	$Cs_{0.1}(MA_{0.17}FA_{0.83})_{0.9}PbBr_{0.33}I_{2.67}$ (NIR, 750 nm), $Cs_{0.1}(MA_{0.17}FA_{0.83})_{0.9}PbBr_{2.97}I_{0.03}$ (green, 569 nm), $Cs_{0.1}(MA_{0.17}FA_{0.83})_{0.9}PbCl_{1.5}Br_{1.5}$ (blue, 475 nm), $CsPbBr_3$, $MAPbBr_3$	$L_{50} \approx 160$ min (NIR), $L > L_0$ for > 475 min (green), $L_{50} < 150$ min (blue) $L_{50} \approx 450$ min ($CsPbBr_3$) $L_{50} \approx 300$ min ($MAPbBr_3$)	$R_0 = 93.34$ W sr^{-1} cm^{-2} (NIR), $L_0 = 736.7$ cd m^{-2} (green), 374.5 cd m^{-2} (blue), 1000 cd m^{-2} ($CsPbBr_3$, $MAPbBr_3$)
He and co-workers[131]	2017/02	ITO/PEDOT:PSS/PVK/ MHP/TPBI/Ca/Al	$Cs_{0.4}MA_{0.6}PbBr_3$	$L_{50} \approx 160$ s	At 30 mA cm^{-2}
Rand and co-workers[34]	2017/03	ITO/poly-TPD or PVK/ MHP/TPBI/LiF/Al	4-fluorophenylmethylammonium iodide (FPMAI):$MAPbI_3$ = 20:100 (NIR)	$L > L_0$ for >10 h (NIR)	At 3 mA cm^{-2}
			PEABr:$MAPbBr_3$ = 20:100 (green)	$L_{60} \approx 15$ min (green)	
Lee and co-workers[35]	2017/03	ITO/PEDOT:PSS/MHP/TPBI/LiF/Al	$MAPbBr_3$	$L_{50} \approx 100$ s	At 6.5 V
Sun and co-workers[158]	2017/03	ITO/PEDOT:PSS/TFB/MHP/TPBI/LiF/Al	$FA_{0.8}Cs_{0.2}PbBr_3$ NPs	$L_{50} \approx 80$ s	Not reported
Liao and co-workers[51]	2017/03	ITO/PEDOT:PSS/MHP/Ca:ZnO/Al	$MAPbBr_{1.95}I_{1.05}$ (red, 634 nm), $MAPbBr_3$, $MAPbBr_{2.7}I_{0.3}$ (yellow, 580 nm)	$EQE = 0.5EQE_{max}$ at 6.2 h (red), 3.5 h (yellow), 5.7 h (green)	$L_0 \approx 580$ cd m^{-2}, at 25 mA cm^{-2}
Song and co-workers[39]	2017/04	ITO/PEDOT:PSS/MHP/EDA or PEI/ SPW-111/LiF/Al	$MAPbBr_3$	$L_{70} \approx 4$ h	At 20 mA cm^{-2}
Song and co-workers[159]	2017/04	ITO/PEDOT:PSS/PVK/ MHP/TPBI/LiF/Al	$CsPbBr_3$ NPs:PMMA	$L_{50} \approx 50$ min	Unencapsulated, under ambient condition (RH = 55%), at 40.7 mA cm^{-2}
Rand and co-workers[52]	2017/04	ITO/poly-TPD/MHP/TPBI/LiF/Al	$MAPbI_3$	$EQE > EQE_0$ for >300 min	At 3 mA cm^{-2}
Song and co-workers[74]	2017/04	ITO/NiO/MHP/ZnO/Al	$CsPbBr_3$ NPs	$L_{70} = 1.75$ h	Unencapsulated, under ambient condition (RH = 65%)
Huang and co-workers[160]	2017/04	ITO/ZnO/PEIE/MHP/TFB/MoO_x/Au	NMAI:CsCl:PbI_2 = 2:1:2 (molar ratio) (red, 688 nm)	$L_{50} \approx 5$ h	At 10 mA cm^{-2}
Duhm and co-workers[149]	2017/05	ITO/PEDOT:PSS/MHP/TPBI/LiF/Al	$CsPbBr_3$:PEO = 6:1 (weight ratio)	$L_{80} \approx 80$ h	$L_0 \approx 1000$ cd m^{-2}
Chen and co-workers[161]	2017/05	ITO/PEDOT:PSS/MHP/TPBI/LiF/Al	$CsPbBr_3$	$L_{50} \approx 70$ min	Not reported
Yu and co-workers[162]	2017/05	ITO/MHP/Au	$MAPbBr_3$ microplatelet	$L > L_0$ for >54 h (at −193 °C)	$L_0 \approx 5000$ cd m^{-2}, at 1 mA, measured at cryogenic temperature
Yu and co-workers[119]	2017/05	ITO/MHP/In:Ga	$MAPbBr_3$:PEO:PVP = 100:50:0.25 (weight ratio)	$L_{65} = 630$ min (at −193 °C) $L_{50} < 2$ min (at 25 °C)	$L_0 \approx 100$ cd m^{-2}, measured at cryogenic temperature
Lee and co-workers[7]	2017/06	ITO/PEDOT:PSS:PFI/ MHP/TPBI/LiF/Al	$CsBr:PbBr_2$ = 1.1:1	$L_{50} \approx 34$ min	$L_0 \approx 50$ cd m^{-2}
You and co-workers[130]	2017/06	ITO/ZnO/PVP/MHP/4,4′-*bis*(carbazol-9-yl)biphenyl (CBP)/MoO_3/Al	$Cs_{0.87}MA_{0.13}PbBr_3$:PVP	$L_{50} \approx 1$ h	$L_0 \approx 65$ cd m^{-2}, at 5 V
Vashishtha and Halpert[144]	2017/06	ITO/PEDOT:PSS/poly-TPD/ MHP/TPBI/Al	$CsPbBr_{0.625}I_{2.375}$ NPs (red, 653 nm)	$L_{50} \approx 7$ min	Unencapsulated
Wang and co-workers[163]	2017/07	ITO/PEDOT:PSS:PFI/poly-TPD/MHP/ 1,3,5-*tri*[(3-pyridyl)-phen-3-yl]benzene (TmPyPB)/Liq/Al	$CsPbBr_3$	$L_{50} \approx 38$ min	$L_0 \approx 200$ cd m^{-2}

structural stability of the MHP crystal lattice. $FAPbBr_3$ has a slightly larger lattice constant (5.99 Å) than $MAPbBr_3$ (5.92 Å) because FA^+ cations have a larger ion radius (2.79 Å) than MA^+ cations (2.70 Å).[164,165] Therefore, the inclusion of FA distorts the Pb—Br—Pb bond angle by 15° and increases the space-filling density, which is considered as the origin of the high structural stability.[164] Also, the thermal decomposition onset of $FAPbBr_3$ is ≈50 °C higher than that of $MAPbBr_3$ (decomposition onset ≈ 150 °C for $MAPbBr_3$ and 200 °C for $FAPbBr_3$).[164] Recently, $FAPbBr_3$ PeLEDs have been demonstrated,[40,100,166,167] but their operational stability has not been reported. In contrast, $FAPbI_3$ is thermodynamically unstable: the perovskite black α-phase spontaneously transforms to a nonperovskite yellow δ-phase at room temperature.[11]

$CsPbBr_3$ is an all-inorganic MHP that has isotropic Cs^+ (ion radius = 1.81 Å[165]) as the A-site cation. Due to the absence of the free rotational motions of anisotropic MA^+ and FA^+ cations, $CsPbBr_3$ does not exhibit hot PL emission from long-lived (10^2 ps scale) energetic carriers; this lack implies that the screening of carrier cooling by liquid-like reorientational motions does not exist in $CsPbBr_3$.[19] Also, time-resolved terahertz spectroscopy has revealed that trap-assisted nonradiative recombination in $CsPbBr_3$ NPs is inefficient, and suggests that the surface-trap density is low with very a high charge-carrier mobility of ≈4500 $cm^2\ V^{-1}\ s^{-1}$;[9] this value is much higher than that of $MAPbBr_3$ single crystals (≈115 $cm^2\ V^{-1}\ s^{-1}$).[168] Because of the inorganic nature, $CsPbBr_3$ is much more thermally stable (decomposition onset = 580 °C)[56] than $MAPbBr_3$ and $FAPbBr_3$ (decomposition onset = 150–250 °C) (**Figure 9**A).[56,164] The superior thermal stability of $CsPbBr_3$ was proven by observing the consistency in absorbance spectra of $CsPbBr_3$ films before and after thermal annealing (at 180 °C for 15 min).[169]

Because of the unique combination of the high thermal stability, charge-carrier mobility, and PLQE (≈90% in solution[170]), $CsPbBr_3$ PeLEDs have stimulated high interest.[7,74,112,149,152,153,157,161] The high thermal stability of $CsPbBr_3$ may improve the operational stability of PeLEDs, possibly by suppressing degradation caused by thermal stresses including Joule heating. Durable $CsPbBr_3$ PeLEDs have been produced, in which the luminance continuously increased from $L_0 \approx 100$ cd m^{-2} to $L_0 > 400$ cd m^{-2} for >15 h of operation time (applied current density of 66.67 mA cm^{-2}), whereas $MAPbBr_3$ PeLEDs exhibited much poorer stability (L_{50} = 255 s).[112] Also, $CsPbBr_3$ PeLEDs with operational lifetime ($L_{50} \approx 450$ min) higher than that of $MAPbBr_3$ PeLEDs ($L_{50} \approx 300$ min) have been reported.[157] PeLEDs based on $CsPbBr_3$ NPs with a device structure of Au/p-MgNiO/$CsPbBr_3$ NPs/n-MgZnO/n^+-GaN also had relatively long operational lifetime of $L_{80} \approx 9$ h.[156] The operational lifetime of $CsPbBr_3$ PeLEDs reported by other groups was shorter ($L_{70} \approx 1.75$ h,[74] $L_{50} \approx 70$ min,[161] 33 min,[7] and <10 min[152,153]) than in the abovementioned studies.[112,149,157] This difference indicates that high thermal stability does not always guarantee high operational stability of PeLEDs; the reason is that the main degradation mechanism in PeLEDs is related more to ion migration than to thermal degradation.

Systems with mixed A-site cations have been investigated to overcome the limitations of systems with single A-site cations ($MAPbX_3$, $FAPbX_3$, and $CsPbX_3$) such as spontaneous transformation to nonperovskite phase and material degradation by heat, light incidence, and air exposure.[85,130,131,157,158,171] For example, incorporation of >10 mol% Cs in $FAPbI_3$ prevents the formation of the nonperovskite yellow δ-phase by increasing the entropy of mixing and modifying the tolerance

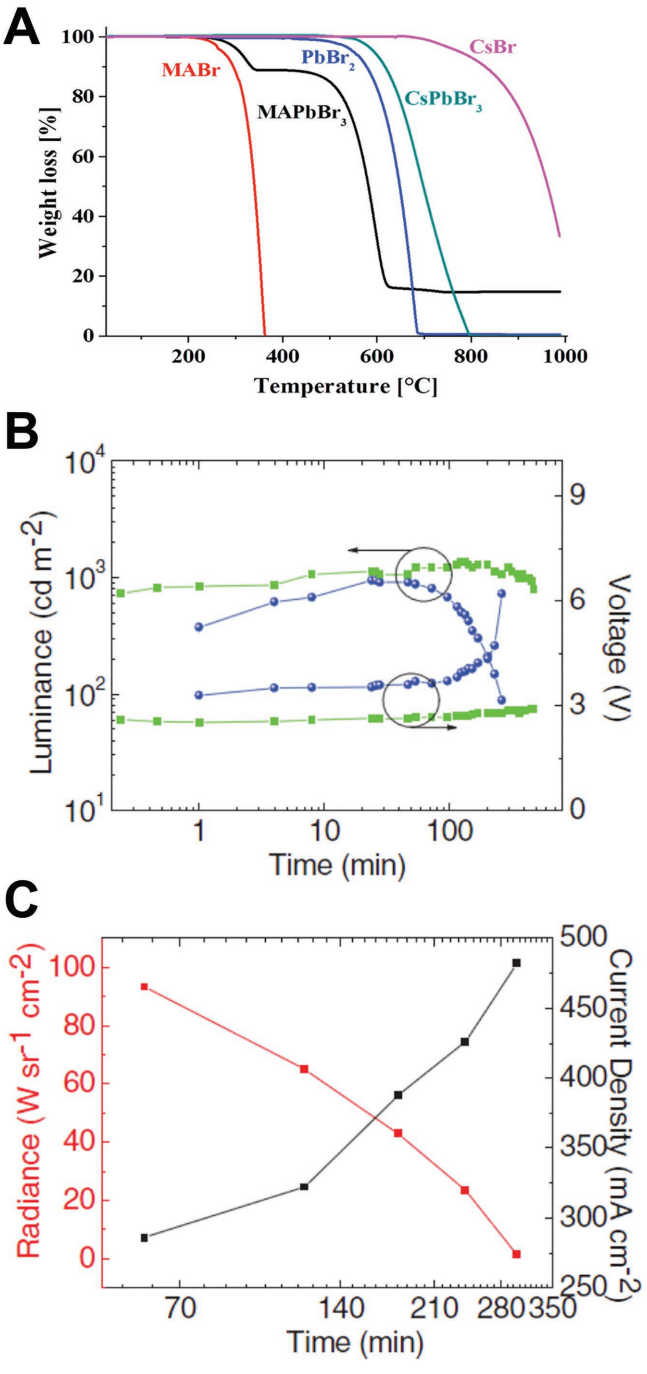

Figure 9. A) Thermogravimetric analysis of MABr, $MAPbBr_3$, $PbBr_2$, $CsPbBr_3$, and CsBr. B,C) Operational lifetime characteristics of green (green points) and blue (blue points) (B) and infrared triple-cation PeLEDs (ITO/ZnO NPs/$Cs_{0.1}(MA_{0.17}FA_{0.83})_{0.9}PbCl_xBr_yI_{3-x-y}$/α-NPD/$MoO_3$/Al) (C). A) Reproduced with permission.[56] Copyright 2015, American Chemical Society. B,C) Reproduced with permission.[157] Copyright 2017, Wiley-VCH.

factor.[44,85,172] Incorporation of Rb can also stabilize the perovskite α-phase of $FAPbI_3$.[172,173] Mixed-cation systems have many advantages for PeLEDs, such as reduced trap density,[85,171] increased charge-carrier mobility,[171] and increased PLQE[158] compared to those of single-cation systems.

Although material stability has been improved by introducing mixed-cation systems, the operational stability of PeLEDs has not been strikingly improved. Green, blue, and infrared PeLEDs based on triple A-site cations (Cs^+, MA^+, and FA^+) have been fabricated;[157] the luminance of the green triple-cation PeLED increased over time from 736.7 to 1335.7 cd m^{-2} for 135 min, then decreased to 800.7 cd m^{-2} at 475 min (Figure 9B), but the operational stabilities of blue and infrared triple-cation PeLEDs were much inferior to that of green triple-cation PeLEDs (Figure 9B,C).[157] Other groups have reported mixed-cation PeLEDs, but they had very short operational lifetimes ($L_{50} \approx 80$ s,[131] 160 s,[158] and >1 h[130]) despite high EL efficiency (33.9 cd A^{-1}).[130]

3.2. Ruddlesden–Popper Phase

To improve the stability of the crystal structure of MHPs, the formation of an RP phase can be a good strategy. To form an RP phase, large OA groups should be added to 3D perovskite structure. The large OA intercalates between the 3D perovskite structures to form an RP multilayered structure (quasi-2D structure). The multilayered structure can be characterized by the number m of PbX_6 octahedral planes, ($m = 1$ for 2D structure and $m = \infty$ for 3D structure) (**Figure 10**A).

RP MHPs have the potential to increase the EL efficiency in PeLEDs, because the exciton binding energy of RP MHPs can be significantly increased by exciton confinement. In RP MHPs that show 2D exciton behaviors, the exciton binding energy can increase to >300 meV,[174–177] which is much higher than that of 3D counterparts (40–150 meV for MAPbBr; 13–50 meV for $MAPbI_3$).[92,178,179] Assuming that all absorbed photons generate electron–hole pairs, the PLQE η can be determined by three different recombination rates: trap-assisted monomolecular recombination rate k_1 (excitonic recombination rate for RP MHPs), bimolecular recombination rate k_2, and Auger recombination rate k_3[180]

$$\eta^{3D} = \frac{nk_2}{k_1 + nk_2 + n^2k_3} \rightarrow \eta^{2D} = \frac{\phi k_1 + nk_2}{k_1 + nk_2 + n^2k_3} \quad (4)$$

where n [cm^{-3}] is the charge-carrier density and ϕ is the ratio of excitonic radiative recombination among all kinds of monomolecular recombination. A recent report calculated that RP MHPs have much higher recombination rates ($k_1 = 5 \times 10^7$ s^{-1}, $k_2 = 2 \times 10^{-9}$ cm^3 s^{-1}, $k_3 = 2 \times 10^{-26}$ cm^6 s^{-1}) than 3D MHPs do ($k_1 = 9 \times 10^5$ s^{-1}, $k_2 = 7 \times 10^{-10}$ cm^3 s^{-1}, $k_3 = 3 \times 10^{-28}$ cm^6 s^{-1}).[180] The higher recombination rates in RP MHPs imply that light emission is more efficient in RP MHPs, and that it originates from excitonic recombination, as well as bimolecular recombination, whereas the contribution of Auger recombination at high n is also larger than that in 3D MHPs. Also, the RP MHPs undergo an energy-transfer process. After recombination of injected electrons and holes in RP-phase MHP crystals, but before quenching, the excitons can be transferred to adjacent crystals that have higher m and a smaller bandgap; as a result, the light is emitted by the crystals that have the highest m (Figure 10A).[3,33,180] This energy-transfer process is attributed to the adjacently positioned RP-phase crystals with different m, and to very fast energy transfer (≈0.5 ps).[180] The energy transfer can be beneficial for EL efficiency because the charge carriers are more concentrated at the crystals that have the highest m and because trap states need to be filled only in the crystals that have the highest m.[3]

RP MHPs can also improve the stability of MHP materials and PeLEDs. RP MHPs have a higher formation energy than that of their 3D counterparts because of a strong van der Waals' force between the large OA groups in RP MHPs, and they thereby have improved material stability at room temperature.[181] Also, these large OA groups can suppress ion migration between 3D MHP multilayers.

The fabrication of RP MHP films is simple; they can be made by just mixing a large OA with a 3D perovskite precursor solution, and then spin-coating the mixed solutions. Based on the advantages (high exciton binding energy, high structural stability, and simple fabrication process), RP PeLEDs have been studied to achieve high EL efficiency and high operational stability.[3,5,33,160,182,183] Infrared PeLEDs that have an RP structure fabricated by mixing $MAPbI_3$ and phenylethylammonium (PEA) iodide showed an EQE_{max} of 8.4%. In addition, the absorption spectrum of RP MHP films did not change much at high RH = 90% for 50 d, whereas the absorption spectrum of 3D MHP films significantly changed after 7 d (Figure 10B); this result demonstrates the high stability of RP MHP films in ambient conditions.[3] RP infrared PeLEDs based on $FAPbI_3$ and 1-naphthylmethylamine iodide (NMAI) showed an EQE_{max} of 11.7% with an improved operational lifetime. The operational lifetime of RP PeLEDs was $L_{50} = 2$ h, which was much better than that of 3D $FAPbI_3$ PeLEDs ($L_{50} = 1$ min).[5] RP PeLEDs based on NMAI and $CsPbI_3$ achieved an EQE_{max} of 3.7% and an operation lifetime of $L_{50} = 5$ h (Figure 10C).[160] Also, RP MHP films showed higher photostability than 3D MHP films did.[155] The PL intensity of RP MHP films (butylammonium-incorporated $MAPbX_3$) was quite stable; it decreased only by ≈10% under irradiation of ≈10 mW cm^{-2}, whereas the PL of 3D MHP films was totally quenched after only 50 s of irradiation. In contrast, the EL intensity of RP PeLEDs decreased very rapidly ($L_{50} \approx 80$ s).[155] RP MHP films in octylammonium–MA mixed systems also had high photostability.[184]

3.3. Suppression of Ion Migration with Additives and Blocking Layers

Because the degradation in PeLEDs is mainly related to electric-field-induced ion migration from MHP emission layers to interfaces and other layers, the suppression of ion migration can be a very effective method to increase the stability of PeLEDs. Because ion migration is a temperature-activated process, the reduction of temperature is the most effective solution,[119,162] but it is not compatible with practical applications of PeLEDs at

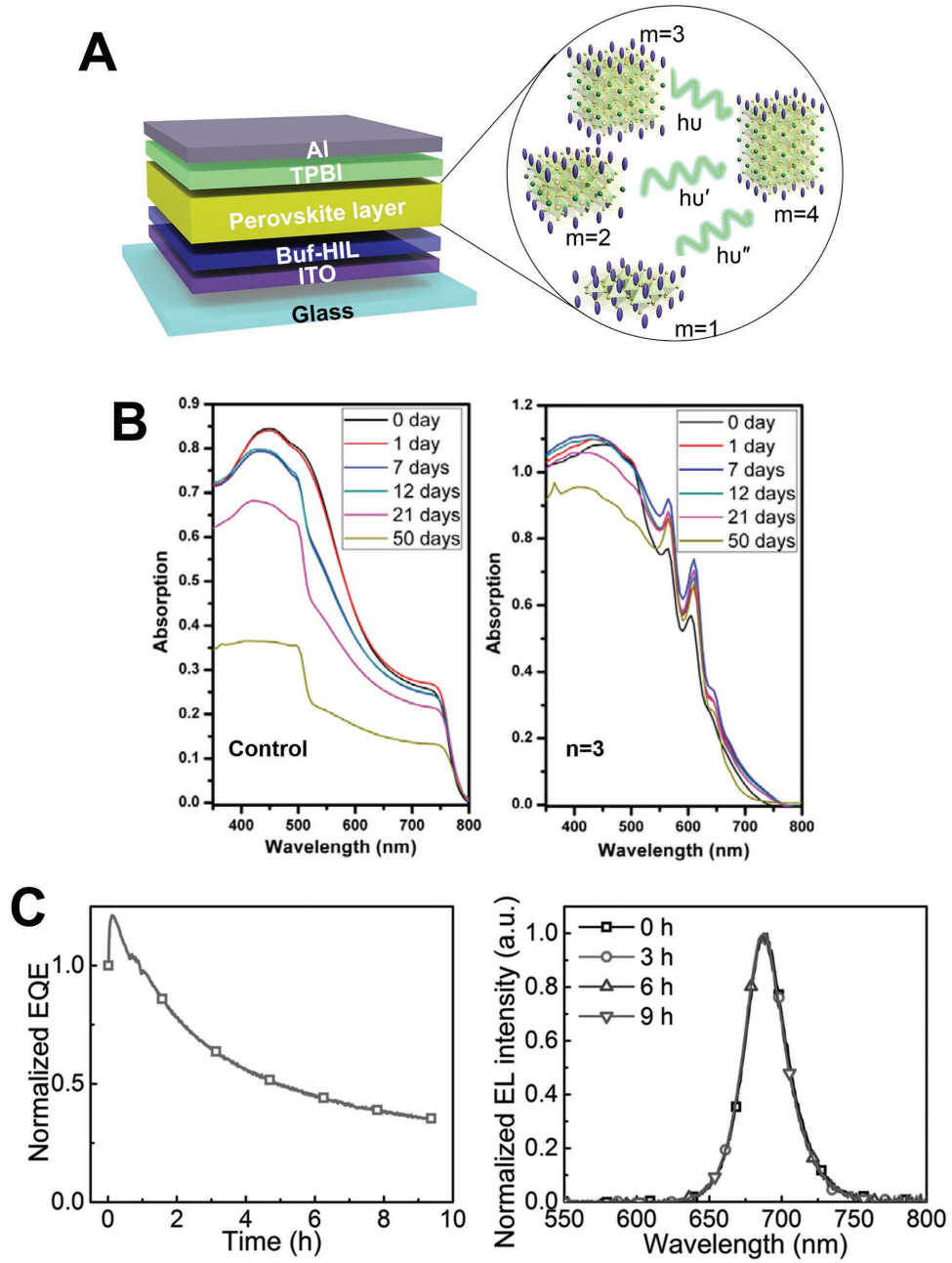

Figure 10. A) Schematic illustration showing device structure of an RP PeLED (ITO/Buf-HIL/$(PEA)_2(MA)_{m-1}Pb_mBr_{3m+1}$/TPBI/LiF/Al) and the energy-transfer process between MHP crystals with different *m*. B) Time evolution of the absorption spectra of 3D ($MAPbI_3$, left) and RP ($(PEA)_2(MA)_2Pb_3I_{10}$, right) MHP films stored in ambient condition (RH = 90%). C) Changes in normalized EQE (left) and EL spectra (right) of a red RP PeLED (ITO/ZnO/polyethylenimine ethoxylated (PEIE)/$(NMA)_2Cs_{m-1}Pb_m(Cl_xI_{1-x})_{3m+1}$/TFB/$MoO_x$/Au) with operational time. A) Reproduced with permission.[33] Copyright 2016, Wiley-VCH. B) Reproduced with permission.[3] Copyright 2016, Nature Publishing Group. C) Reproduced with permission.[160] Copyright 2017, Wiley-VCH.

room temperature. RP phase (Section 3.2) can also be an effective method to inhibit ion migration.

Another feasible strategy to suppress ion migration is to introduce ion-blocking interlayers. They can suppress ion migration by spatially blocking the migrating ions and passivating defects at grain boundaries and interfaces.[39,114,129,130] Lewis bases that have electron-donating groups are good candidates for passivating agents.[82]

An amine-based small molecule (ethylenediamine (EDA)) and an amine-based polymer (polyethylenimine (PEI)) have been used as passivating agents for $MAPbBr_3$.[39] EDA and PEI were spin-coated on top of $MAPbBr_3$ layers, and their penetration depths were analyzed by performing TOF-SIMS. EDA penetrated more deeply than PEI, and therefore more effectively passivated the defects of $MAPbBr_3$ than PEI did; the passivation effect extended PL lifetime and reduced PL

blinking. Also, the absence of color change in Ag electrodes (i.e., no formation of AgBr) clearly demonstrated that ion migration was inhibited by EDA and PEI interlayers. Furthermore, as a result of the passivation of defects and reduced ion migration, the operational lifetime of $MAPbBr_3$ PeLEDs was significantly increased; the operational lifetime (L_{70}) of the passivated PeLED was ≈4 h, whereas the luminance of unpassivated PeLED rapidly decreased to <10% at ≈0.7 h (**Figure 11**A).[39]

Nanostructured carbon layers composed of n-doped graphene, carbon dots, and the fullerene derivative phenyl-C_{61}-butyric acid methyl ester (PCBM) have also been developed as ion-blocking layers.[129] The nanostructured carbon layers effectively blocked ion migration from the MHP layers to other layers and diffusion of Ag atoms from electrodes to MHP layers, and also formed an Ohmic contact with electrodes. The MHP films and PeSCs with the nanostructured carbon layers showed much improved photo- and thermal-stability compared to those of MHP films and of PeSCs with conventional PCBM layers.[129]

Dense metal oxide interlayers can provide a barrier that blocks ion migration from MHP layers and atmospheric gas permeation into MHP layers. SnO_x layers formed by atomic-layer deposition on top of Al-doped ZnO electron extraction layers excellently protected $MAPbI_3$ layers from ingress of moisture (water vapor transmission rate = 7×10^{-5} g m^{-2} d^{-1}).[185,186] Furthermore, the SnO_x layers blocked outdiffusion of thermal decomposition products (e.g., hydrogen iodide (HI)) of $MAPbI_3$ and also possibly blocked I^- anion migration from $MAPbI_3$ layers, as evidenced by the suppressed corrosion of Ag electrodes and by the substantially increased operational lifetime of PeSCs.[185] Amine-mediated TiO_x interlayers have been incorporated between Ag electrodes and PCBM layers to hinder the migration of halide anions to Ag electrodes and consequent corrosion of Ag electrodes.[114] Even with Au electrodes that do not easily corrode, the introduction of a Cr metal interlayer between Au electrodes and spiro-MeOTAD increased device stability because the Cr interlayers effectively prevented diffusion of Au atoms into the spiro-MeOTAD and MHP layers.[141] Also, metal fluorides (e.g., BaF_2) that have been used to improve the device lifetime in OLEDs may suppress the diffusion of metallic species from the cathode.[187]

Degradation caused by diffusion of In and Sn atoms from ITO electrodes (etched by PEDOT:PSS) to MHP layers could be overcome by replacing ITO with chemically inert electrodes (e.g., four-layer graphene electrodes) as demonstrated by TOF-SIMS profiles (Figure 11B).[37] Also, a buffer hole-injection layer (Buf-HIL) that is composed of PEDOT:PSS and perfluorinated ionomer (PFI) can block the diffusion of In and Sn atoms.[188] The Buf-HIL, which can increase the hole-injection efficiency and thereby lower the current density at the same luminance in devices, improved the device operational lifetime of polymer LEDs due to the suppressed diffusion of In and Sn atoms and the reduced driving current density (Figure 11C);[188] this can also be definitely applied for PeLEDs.

Incorporation of additives into MHP layers is a useful approach to passivate defects, separate MHP grains, and thereby hinder ion migration. Furthermore, incorporation of additives (e.g., polymers and organic small molecules) to MHPs can facilitate the formation of homogeneous film morphology with reduced pinholes and decrease grain size by

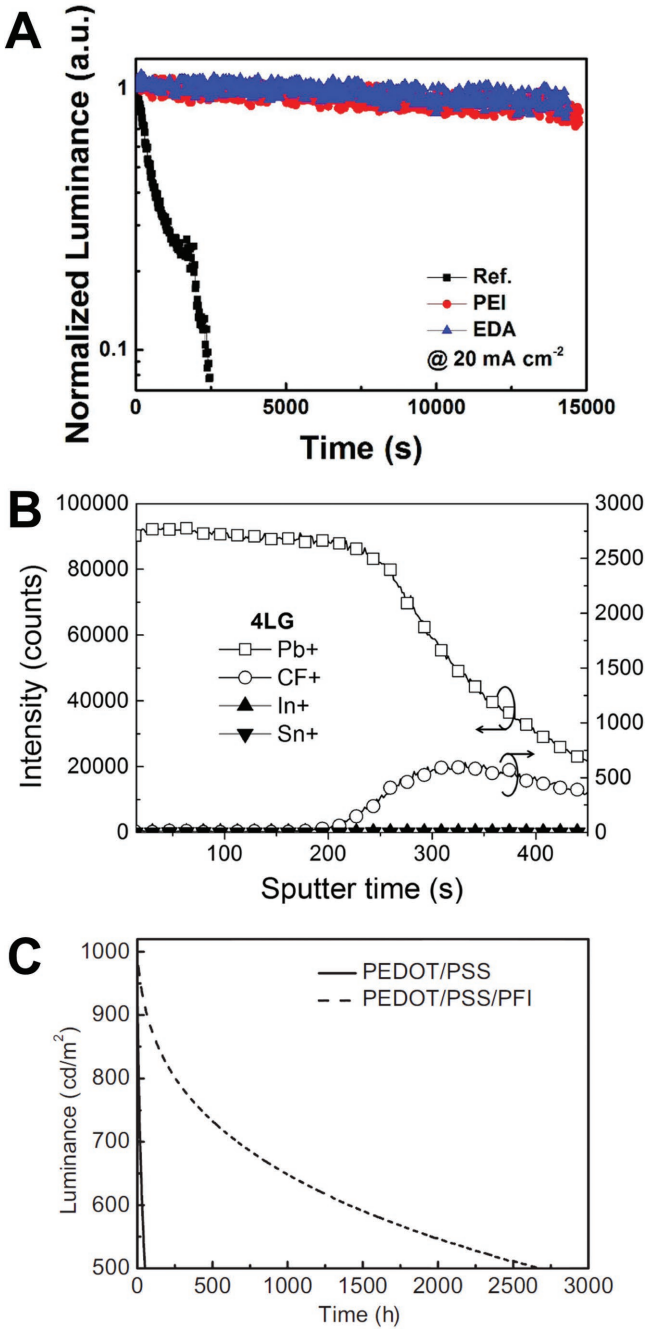

Figure 11. A) Operational lifetime of PeLEDs (ITO/PEDOT:PSS/$MAPbBr_3$/EDA or PEI/SPW-111/LiF/Al) passivated by PEI and EDA. B) TOF-SIMS depth profiles of graphene/Buf-HIL/$MAPbBr_3$ films. C) Operational lifetime of polymer LEDs using PEDOT:PSS or PEDOT:PSS:PFI as a hole-injection layer. A) Reproduced with permission.[39] Copyright 2017, American Chemical Society. B) Reproduced with permission.[37] Copyright 2017, Wiley-VCH. C) Reproduced with permission.[188] Copyright 2007, Wiley-VCH.

forming a matrix for MHP grains and inhibiting MHP grain growth;[1,73,189] these are desirable characteristics for high-efficiency PeLEDs. However, decreased grain size corresponds to an increase in the number of grain boundaries (defect sites); this change might degrade the operational stability of

PeLEDs. Therefore, the additives should have electron-donating groups that can passivate defects to mitigate this detrimental effect. Also, the proportion between the MHP and the additive must be well optimized because an excessive amount of insulating additives can impede charge injection and transport. The choice of additives for MHP layers is somewhat limited because the additives must be completely dissolved into MHP solutions, in which polar aprotic solvents such as dimethylformamide (DMF) and dimethyl sulfoxide are typically used.

The stability of $CsPbBr_3$ PeLEDs can be increased by incorporating a polymer additive (PEO) to $CsPbBr_3$.[149] $CsPbBr_3$–PEO composite films with grains of a few micrometers in size were fabricated by spin-coating with chloroform steam post-treatment; PeLEDs that used them had both high EL efficiency (21.38 cd A^{-1}) and high operational stability ($L_{80} \approx 80$ h), which were both higher those of pure $CsPbBr_3$ PeLEDs (8.78 cd A^{-1}; $L_{80} \approx 20$ h).[149] However, PEO is an ion-conducting polymer, so the stability increase was not definitely a result of suppression of ion migration.[132]

Poly(ethylene glycol) (PEG) has also been used as a polymer scaffold for making stable MHP layers.[189] Because of the hygroscopic nature of PEG and the formation of hydrogen bonding between PEG molecules and MHP grains, the $MAPbI_3$–PEG composite films strongly resisted degradation by moisture and light soaking, and even showed self-healing behavior, i.e., a spontaneous rapid recovery of the perovskite phase under water-vapor spray. Also, methylamine (CH_3NH_2) solution additives suppress the formation of I_2, and result in MHP films with reduced defect density, so ion migration is impeded.[190]

3.4. Fabrication of Uniform Bulk Polycrystalline MHP Layers

Partial film coverage of MHP emission layers in PeLEDs can allow the formation of low-resistance shunting paths that pass unwanted leakage current, which causes significant EL efficiency drop and fast degradation of devices.[1,7] Therefore, one of the most important aims in PeLED studies is to fabricate uniform, pinhole-free MHP emission layers. However, achieving uniform MHP layers by common spin-coating is difficult because MHP grains are coarsened easily and spontaneously form nonuniform films.[1,7,36]

Representative strategies to make uniform MHP layers are nanocrystal pinning[1] and modification of the underlying layers.[7,30] The goal of nanocrystal pinning is to fabricate uniform MHP films and reduce MHP grain size by dripping nonpolar solvents (e.g., chloroform, toluene, chlorobenzene) on the spinning layers and thereby induce immediate crystallization. Because of the simplicity of the process, nanocrystal pinning has been widely used to fabricate uniform MHP films.[1,31,34–37,51] Also, uniform $MAPbBr_3$ NP and $CsPbBr_3$ layers could be fabricated by using a Buf-HIL (PEDOT:PSS:PFI) as the underlying hole-injection layer.[7,30] The MHP layers formed on the Buf-HIL were uniform with closely packed grains, whereas the MHP layers formed on PEDOT:PSS were sparse and nonuniform;[7,30] the difference in morphology could be explained by partial dissolution of PFI into the MHP solution during spin-coating; the dissolved PFI molecules could increase the number of nucleation sites by inducing heterogeneous nucleation, and decrease the MHP grain size by inhibiting growth of MHP grains.[7] A uniform morphology of the MHP layers was also achieved by MA-vapor treatment,[36] by incorporation of HBr[32,154] or polymers[73] to MHP precursor solutions, and by double spin-coating of MHP precursor solutions.[51]

3.5. Diverse Approaches to Make Stable MHP NPs

Although MHP NPs are capped with organic ligands that passivate surface defects and increase the stability of NPs in colloidal solutions, the ionic crystal structure of MHP NPs still provides low stability of the NPs under moisture and heat treatment, and in polar solvent and film states.

Many research groups have reported methods to improve the stability of MHP NPs.[98,101,103,105,107–109,145,150,191–193] Song et al. and Li et al. proved that all-inorganic $CsPbBr_3$ NPs are much more stable than $MAPbBr_3$ NPs in the solution state even though $CsPbBr_3$ NPs were synthesized at room temperature in ambient condition; $CsPbBr_3$ NP solutions maintained high PLQE (>80%) for >30 d, but $MAPbBr_3$ NP solutions showed dramatically reduced PLQE (<10%) in <5 d; the reasons for this high stability of $CsPbBr_3$ NP solutions[98,103] compared to that of $MAPbBr_3$ NP solutions have not yet been elucidated. Although $CsPbBr_3$ NPs showed long-lasting high PLQE in solution states, their PLQE dramatically decreased in the film state.[105] For application to LEDs, colloidal NPs should be coated into a film state and maintain high PLQE in that state. Highly monodispersed $FAPbBr_3$ NPs that maintain high PLQE (≈80%) in the film state at elevated temperature (50 °C) have been reported, but $CsPbBr_3$ NPs showed dramatically reduced PLQE (<10%) in the film state at 50 °C.[105] However, these MHP NPs still showed low stability in polar organic solvents and moisture, and also they aggregated readily during film formation.

Ligand-engineering methods that passivate the surface of MHP NPs with large organic ligands to improve the stability of NPs in polar organic solvents and moisture have been demonstrated. MHP NPs have been passivated using polyhedral oligomeric silsesquioxane (POSS), which is a cage-like molecule with an inorganic siloxane core and eight organic corner groups.[191] POSS can act as a protective ligand matrix that prevents water penetration into the core MHP NPs and undesirable anion exchange. POSS with strong steric hindrance can also prevent the aggregation of MHP NPs and maintain the original shape of NPs in film states.

MHP NPs can be capped with branched capping ligands, (3-aminopropyl) triethoxysilane (APTES) and amino-functionalized polyhedral oligomeric silsesquioxane (NH_2—POSS).[107] APTES-capped MHP NPs had high stability and showed slightly reduced PL intensity in various protic solvents for 2.5 h (≈100% for NPs in methanol, and ≈70% for NPs in ethanol and isopropyl alcohol compared to the initial PL intensity), however, NPs capped by linear organic ligands (i.e., oleic acid, octylammonium bromide) did not show any emission in protic solvents; these results indicate that strong steric hindrance and the hydrolysis properties of APTES efficiently prohibit the penetration of protic solvents into the core NPs. APTES can also prevent redissolution of as-formed MHP NPs into DMF solvent, and thus preserve the original shape and properties.

Recently, MHP NPs with thermally crosslinkable and polymerizable ligands, 4-vinylbenzyl-dimethyloctadecylammonium chloride (V18) have been reported (**Figure 12**A).[150] The styryl group in V18 allows crosslinking between MHP NPs; the crosslinked NPs based on V18 maintained high PLQE very well (≈100% of initial PL intensity in ambient condition for one month and >80% of initial PL intensity in moisture for 120 min); in contrast, octylammonium-bromide-based un-crosslinked NPs showed rapid decrease of PLQE (≈65% of the initial PL intensity in ambient conditions for one month and ≈70% of the initial PL intensity in moisture for 120 min).

Fabricating MHP NP–polymer composite films can also be a good strategy to increase the stability of the NPs. MHP NP–polymer composite films have been composed of various polymers such as polystyrene, poly(methyl methacrylate), PVDF, polycarbonate, acrylonitrile butadiene styrene, cellulose acetate, poly(vinyl chloride), and ethyl cellulose;[108,150,159,192,193] due to the good dispersion and efficient surface passivation of NPs in the polymer matrix, these composite films have shown high stability in water, and efficient radiative recombination of geminate charges. The styryl group in V18 induces radical polymerization with other monomers (styrene and methyl methacrylate), and consequently formed polymer–V18–NP composites that were highly stable in water for >90 d (Figure 12B).[150] MHP NP–hydrophobic semicrystalline polymer (PVDF) composite films have good solubility in organic solvents and strong interaction between CF_2 groups in PVDF and NH_3^+ group in NPs;[108,192,193] as a result, color-tunable NP–PVDF composite films could be easily fabricated; they maintained high PLQE under UV irradiation (≈63% of the initial PLQE) and water (≈68% of the initial PLQE), which are similar to the PLQE of films without UV and water (≈70% of the initial PLQE).[108,192,193]

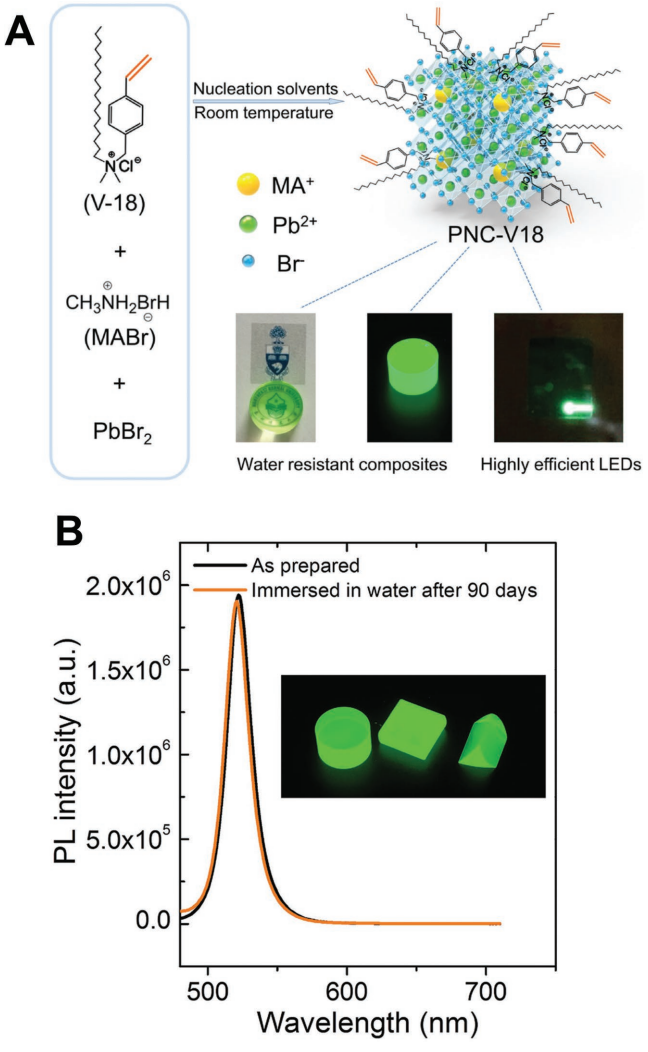

Figure 12. A) The design of MHP NPs using V18 as a crosslinking agent and their applications. B) PL intensity of an as-prepared MHP NP–V18–polymer composite and the same composite after immersion in water for 90 d. Reproduced with permission.[150] Copyright 2017, Wiley-VCH.

Postligand engineering is used to exchange or remove the ligand of the NPs after the synthesis process, but can also affect the stability of MHP NPs. Methods that have been tested to increase the luminescence efficiencies of MHP NP-based PeLEDs include replacing long ligands (here, oleylamine and oleic acid) with shorter ligands[101] and reducing the concentration of surface ligands by ligand postengineering.[109] However, the ligand-exchange step and excess removal of surface ligands may destabilize the MHP NPs in solution and thereby reduce both the PLQE and the stability. Thus, to improve the stability, the method of exchanging or removing ligands from the surface of MHP NPs must be chosen carefully. Crosslinking surface ligands on MHP NPs by depositing hydroxide-terminated aluminum oxide can link the NPs and make them insoluble in organic solvents.[145] These crosslinked NPs were not washed off by the organic solvents, and also showed improved PLQE because their surface defects were passivated by alumina.

4. Summary and Outlook

We have reviewed the origins of the low stability of PeLEDs by categorizing the origins into instability: (i) of MHP materials (the influence of crystal structure, temperature, atmosphere, photoexcitation on stability, and colloidal instability) and (ii) of PeLED devices (each constituent layer and interface). Then, we reviewed recent progress in reducing these instabilities. The cubic perovskite structure is the most stable phase in MHPs and forms when $0.813 \leq t_f \leq 1.107$ and $0.442 \leq o_c \leq 0.895$. Thermal degradation occurs even at moderate annealing temperature (≈85 °C) and is severe, especially for $MAPbX_3$, due to its thermodynamic instability. This thermal instability can be mitigated by using thermally stable A-site cations (FA^+ and Cs^+). The influence of oxygen on the luminescent properties is still controversial; the general opinion is that light-induced formation of O_2^- causes decomposition of MHPs. Degradation can be accelerated by hydration of MHPs under a humid atmosphere, and by exposure to light. These instabilities under atmosphere and light exposure can be overcome by using layered perovskite structures (RP MHPs) and cladding layers.

Degradation of PeLEDs is mainly ascribed to the migration of halide anions in response to an electrical field; the migration causes irreversible degradation from the interfaces, the

corrosion of metal electrodes, and the generation of defects inside the MHP layers. Also, the formation of a p–i–n junction in the MHP layers might be related to the degradation. Diffusion of metal atoms from electrodes can induce the degradation of PeLEDs by providing shunting paths and nonradiative recombination sites. Color instability of PeLEDs, which is caused by easy ion migration and the presence of a miscibility gap, is also reviewed. Similar to the solutions for instabilities under atmosphere and light exposure, instability caused by ion migration can be mitigated by introducing layered perovskite structures and ion-blocking interlayers and additives. The device stability can be further enhanced by forming uniform MHP layers.

The factors that limit the operational stability of PeLEDs based on MHP NPs are identified, and strategies to make stable MHP NPs are reviewed; the strategies include A-site cation engineering, ligand engineering, and use of MHP NP–polymer composites.

We also suggest future research directions for achieving high-stability PeLEDs. First, to extend the operational lifetime of PeLEDs, the suitability of strategies to remove the electric-field-induced ion migration should be increased. Although RP MHPs have been studied as a fundamental solution to improve both the EL efficiency and the device stability, the reported operational lifetimes of RP PeLEDs are just several hours,[160] which is much shorter than that of OLEDs. This poor PeLED stability can be ascribed to a lack of understanding of the optimal RP phase; we must determine which chemical structure of large-sized OA is the best for achieving efficient exciton confinement, defect passivation, and prevention of ion migration while retaining moderate charge-transport ability. For example, we must first identify the best chemical structure of large OA among aliphatic structures, aromatic structures, and their combinations, and determine the functional groups that can passivate defect sites most efficiently.

Study of the passivation of MHP grains is also imperative to improve device stability. To prevent ion migration in PeLEDs based on bulk polycrystalline MHP emission layers (which are formed by the coating of MHP precursor solutions), efficient ion-blocking materials must be developed. Because the MHP grain size in PeLEDs should be decreased to spatially confine charge carriers and thereby enhance radiative recombination,[1] a concomitantly increased grain-boundary area (a main pathway for ion migration[121]) should be passivated with ion-blocking materials. Ideally, these ion-blocking materials should perfectly surround the MHP grains and passivate all the defects at the surface of the MHP grains (or at the grain boundaries) without losing efficient charge injection into the MHP grains. For this purpose, the development of core–shell-type colloidal MHP NPs can also be an effective strategy. These ion-blocking materials or shell materials need not to be insulating; semiconducting materials might be a better choice to improve charge injection and transport in devices.

Inspired by the history of OLEDs, vacuum deposition of MHP layers may increase the operational stability of PeLEDs because vacuum deposition may form dense MHP layers. In OLEDs, vacuum deposition yields more dense organic layers with fewer trap states than solution processes do.[194] However, vacuum deposition of MAX is challenging due to a difficulty of the control of the deposition rate.[195] Instead, the vacuum deposition rate of Cs-based MHPs can be controlled more easily due to their high evaporation temperature. Therefore, dual-source deposition of CsX and PbX_2 and flash evaporation of $CsPbX_3$ can be promising approaches to fabricate compact $CsPbX_3$ emission layers in PeLEDs.

Furthermore, degradation of PeLEDs can be retarded by changing the operation conditions. The use of a pulsed-current-mode operation combined with negative pulses rather than DC-mode operation may improve the device stability of PeLEDs. The pulsed or alternating-current (AC)-mode operation in OLEDs or AC EL devices has been considered to increase the operational lifetime because frequent reversal of the applied voltage can prevent charge accumulation at interfaces in OLEDs, and dielectric layers in AC EL devices (which are absent in DC-driven OLEDs) can suppress side reactions between electrodes and emission layers and block ingress of moisture and oxygen.[196–198] In PeLEDs or perovskite AC EL devices, the pulsed or AC-mode operation can be more effective to improve device stability than in OLEDs because AC-driven PeLEDs can avoid accumulation of migrated ions (which have escaped from the MHP lattice) at interfaces, and the dielectric layers in perovskite AC EL devices can also block ion migration.

For display applications of PeLEDs, red, green, and blue PeLEDs with high efficiency and stability must be realized. The color of PeLEDs can be simply tuned by substitution of halogen anions,[15] but tuning the color with substitution of halogen anions may result in low efficiency of the PeLEDs, especially for blue PeLEDs based on Cl^- anions.[103] The low efficiency of blue PeLEDs based on Cl^- anions (e.g., CE_{max} = 0.14 cd A^{-1})[103] is due to the low PLQE and to phase separation caused by migration of halide anions. We suggest that RP MHPs can substantially contribute to the realization of high-efficiency multicolored PeLEDs. In RP MHPs, exciton confinement causes an increase in the bandgap as m decreases, so the blueshift in the emission spectrum can be controlled by adjusting the amount of large OA. For example, $CsPbBr_3$ mixed with 4-phenylbutylammonium bromide showed a PL emission peak at 475 nm which is blueshifted by ≈52 nm compared to the peak of 3D $CsPbBr_3$ (527 nm).[183] Therefore, the color of PeLEDs can be further precisely tuned in combination with halide anion substitution. Combined with other advantages such as increased exciton binding energy, reduced trap density, and the ability to prevent ion migration, the color tunability of RP MHPs provides the possibility of high-efficiency blue and sky-blue PeLEDs.

The industrialization of PeLEDs may be imminent. Although the operational stability of PeLEDs must still be further improved, we believe that the instability will be overcome eventually because the major degradation mechanisms are known. Furthermore, MHP NP emitters themselves might be commercialized much earlier than PeLEDs because the MHP NPs can be used in photoluminescent color filters with their remarkably high color purity for downconversion of an excitation light source.[97,199] From this work here, researchers should gain insight into recent studies, and eventually contribute to the development of high-stability PeLEDs.

Acknowledgements

This work was supported by the National Research Foundation of Korea (NRF) grant funded by the Korea government (MSIT) (NRF-2016R1A3B1908431).

Conflict of Interest

The authors declare no conflict of interest.

Keywords

device lifetime, ion diffusion, long-term stability, next-generation emitters, organic–inorganic hybrid perovskites

Received: August 13, 2017
Revised: October 14, 2017
Published online: January 25, 2018

[1] H. Cho, S.-H. Jeong, M.-H. Park, Y.-H. Kim, C. Wolf, C.-L. Lee, J. H. Heo, A. Sadhanala, N. Myoung, S. Yoo, S. H. Im, R. H. Friend, T.-W. Lee, *Science* **2015**, *350*, 1222.
[2] a) Y.-H. Kim, H. Cho, T.-W. Lee, *Proc. Natl. Acad. Sci. USA* **2016**, *113*, 11694; b) M.-H. Park, S.-H. Jeong, H.-K. Seo, C. Wolf, Y.-H. Kim, H. Kim, J. Byun, J. S. Kim, H. Cho, T.-W. Lee, *Nano Energy* **2017**, *42*, 157.
[3] M. Yuan, L. N. Quan, R. Comin, G. Walters, R. Sabatini, O. Voznyy, S. Hoogland, Y. Zhao, E. M. Beauregard, P. Kanjanaboos, Z. Lu, D. H. Kim, E. H. Sargent, *Nat. Nanotechnol.* **2016**, *11*, 872.
[4] Z. Xiao, R. A. Kerner, L. Zhao, N. L. Tran, K. M. Lee, T.-W. Koh, G. D. Scholes, B. P. Rand, *Nat. Photonics* **2017**, *11*, 108.
[5] N. Wang, L. Cheng, R. Ge, S. Zhang, Y. Miao, W. Zou, C. Yi, Y. Sun, Y. Cao, R. Yang, Y. Wei, Q. Guo, Y. Ke, M. Yu, Y. Jin, Y. Liu, Q. Ding, D. Di, L. Yang, G. Xing, H. Tian, C. Jin, F. Gao, R. H. Friend, J. Wang, W. Huang, *Nat. Photonics* **2016**, *10*, 699.
[6] L. Protesescu, S. Yakunin, M. I. Bodnarchuk, F. Krieg, R. Caputo, C. H. Hendon, R. X. Yang, A. Walsh, M. V. Kovalenko, *Nano Lett.* **2015**, *15*, 3692.
[7] H. Cho, C. Wolf, J. S. Kim, H. J. Yun, J. S. Bae, H. Kim, J.-M. Heo, S. Ahn, T.-W. Lee, *Adv. Mater.* **2017**, *29*, 1700579.
[8] C. C. Stoumpos, C. D. Malliakas, J. A. Peters, Z. Liu, M. Sebastian, J. Im, T. C. Chasapis, A. C. Wibowo, D. Y. Chung, A. J. Freeman, B. W. Wessels, M. G. Kanatzidis, *Cryst. Growth Des.* **2013**, *13*, 2722.
[9] G. R. Yettapu, D. Talukdar, S. Sarkar, A. Swarnkar, A. Nag, P. Ghosh, P. Mandal, *Nano Lett.* **2016**, *16*, 4838.
[10] T. M. Brenner, D. A. Egger, A. M. Rappe, L. Kronik, G. Hodes, D. Cahen, *J. Phys. Chem. Lett.* **2015**, *6*, 4754.
[11] A. A. Zhumekenov, M. I. Saidaminov, M. A. Haque, E. Alarousu, S. P. Sarmah, B. Murali, I. Dursun, X.-H. Miao, A. L. Abdelhady, T. Wu, O. F. Mohammed, O. M. Bakr, *ACS Energy Lett.* **2016**, *1*, 32.
[12] A. Sadhanala, F. Deschler, T. H. Thomas, S. E. Dutton, K. C. Goedel, F. C. Hanusch, M. L. Lai, U. Steiner, T. Bein, P. Docampo, D. Cahen, R. H. Friend, *J. Phys. Chem. Lett.* **2014**, *5*, 2501.
[13] C. Wolf, J.-S. Kim, T.-W. Lee, *ACS Appl. Mater. Interfaces* **2017**, *9*, 10344.
[14] Z.-K. Tan, R. S. Moghaddam, M. L. Lai, P. Docampo, R. Higler, F. Deschler, M. Price, A. Sadhanala, L. M. Pazos, D. Credgington, F. Hanusch, T. Bein, H. J. Snaith, R. H. Friend, *Nat. Nanotechnol.* **2014**, *9*, 687.
[15] Y.-H. Kim, H. Cho, J. H. Heo, T.-S. Kim, N. Myoung, C.-L. Lee, S. H. Im, T.-W. Lee, *Adv. Mater.* **2015**, *27*, 1248.
[16] T. Hattori, T. Taira, M. Era, T. Tsutsui, S. Saito, *Chem. Phys. Lett.* **1996**, *254*, 103.
[17] K. Chondroudis, D. B. Mitzi, *Chem. Mater.* **1999**, *11*, 3028.
[18] I. Koutselas, P. Bampoulis, E. Maratou, T. Evagelinou, G. Pagona, G. C. Papavassiliou, *J. Phys. Chem. C* **2011**, *115*, 8475.
[19] H. Zhu, K. Miyata, Y. Fu, J. Wang, P. P. Joshi, D. Niesner, K. W. Williams, S. Jin, X.-Y. Zhu, *Science* **2016**, *353*, 1409.
[20] Z.-G. Yu, *J. Phys. Chem. Lett.* **2016**, *7*, 3078.
[21] A. Benor, S. Takizawa, C. Pérez-Bolivar, P. Anzenbacher Jr., *Appl. Phys. Lett.* **2010**, *96*, 243310.
[22] T.-H. Han, Y. Lee, M.-R. Choi, S.-H. Woo, S.-H. Bae, B. H. Hong, J.-H. Ahn, T.-W. Lee, *Nat. Photonics* **2012**, *6*, 105.
[23] T.-H. Han, M.-H. Park, S.-J. Kwon, S.-H. Bae, H.-K. Seo, H. Cho, J.-H. Ahn, T.-W. Lee, *NPG Asia Mater.* **2016**, *8*, e303.
[24] Y.-H. Kim, C. Wolf, H. Cho, S.-H. Jeong, T.-W. Lee, *Adv. Mater.* **2016**, *28*, 734.
[25] M.-H. Park, T.-H. Han, Y.-H. Kim, S.-H. Jeong, Y. Lee, H.-K. Seo, H. Cho, T.-W. Lee, *J. Photonics Energy* **2015**, *5*, 53599.
[26] X. Dai, Y. Deng, X. Peng, Y. Jin, *Adv. Mater.* **2017**, *29*, 1607022.
[27] W. S. Yang, J. H. Noh, N. J. Jeon, Y. C. Kim, S. Ryu, J. Seo, S. Il Seok, *Science* **2015**, *348*, 1234.
[28] N. J. Jeon, J. H. Noh, W. S. Yang, Y. C. Kim, S. Ryu, J. Seo, S. Il Seok, *Nature* **2014**, *517*, 476.
[29] H. Kim, K.-G. Lim, T.-W. Lee, *Energy Environ. Sci.* **2016**, *9*, 12.
[30] Y.-H. Kim, C. Wolf, Y.-T. Kim, H. Cho, W. Kwon, S. Do, A. Sadhanala, C. G. Park, S.-W. Rhee, S. H. Im, R. H. Friend, T.-W. Lee, *ACS Nano* **2017**, *11*, 6586.
[31] J. C. Yu, D. W. Kim, D. B. Kim, E. D. Jung, K.-S. Lee, S. Lee, D. Di Nuzzo, J.-S. Kim, M. H. Song, *Nanoscale* **2017**, *9*, 2088.
[32] J. C. Yu, D. B. Kim, E. D. Jung, B. R. Lee, M. H. Song, *Nanoscale* **2016**, *8*, 7036.
[33] J. Byun, H. Cho, C. Wolf, M. Jang, A. Sadhanala, R. H. Friend, H. Yang, T.-W. Lee, *Adv. Mater.* **2016**, *28*, 7515.
[34] L. Zhao, Y.-W. Yeh, N. L. Tran, F. Wu, Z. Xiao, R. A. Kerner, Y. L. Lin, G. D. Scholes, N. Yao, B. P. Rand, *ACS Nano* **2017**, *11*, 3957.
[35] J. W. Lee, Y. J. Choi, J. M. Yang, S. Ham, S. K. Jeon, J. Y. Lee, Y. H. Song, E. K. Ji, D. H. Yoon, S. Seo, H. Shin, G. S. Han, H. S. Jung, D. Kim, N. G. Park, *ACS Nano* **2017**, *11*, 3311.
[36] Y. K. Chih, J. C. Wang, R. T. Yang, C. C. Liu, Y. C. Chang, Y. S. Fu, W. C. Lai, P. Chen, T. C. Wen, Y. C. Huang, C. S. Tsao, T. F. Guo, *Adv. Mater.* **2016**, *28*, 8687.
[37] H.-K. Seo, H. Kim, J. Lee, M.-H. Park, S.-H. Jeong, Y.-H. Kim, S.-J. Kwon, T.-H. Han, S. Yoo, T.-W. Lee, *Adv. Mater.* **2017**, *29*, 1605587.
[38] S.-H. Jeong, S.-H. Woo, T.-H. Han, M.-H. Park, H. Cho, Y.-H. Kim, H. Cho, H. Kim, S. Yoo, T.-W. Lee, *NPG Asia Mater.* **2017**, *9*, e411.
[39] S. Lee, J. H. Park, B. R. Lee, E. D. Jung, J. C. Yu, D. Di Nuzzo, R. H. Friend, M. H. Song, *J. Phys. Chem. Lett.* **2017**, *8*, 1784.
[40] Y.-H. Kim, G.-H. Lee, Y.-T. Kim, C. Wolf, H. J. Yun, W. Kwon, C. G. Park, T.-W. Lee, *Nano Energy* **2017**, *38*, 51.
[41] N. H. Tiep, Z. Ku, H. J. Fan, *Adv. Energy Mater.* **2016**, *6*, 1501420.
[42] T. A. Berhe, W.-N. Su, C.-H. Chen, C.-J. Pan, J.-H. Cheng, H.-M. Chen, M.-C. Tsai, L.-Y. Chen, A. A. Dubale, B.-J. Hwang, *Energy Environ. Sci.* **2016**, *9*, 323.
[43] H.-S. Kim, J.-Y. Seo, N.-G. Park, *ChemSusChem* **2016**, *9*, 2528.
[44] Z. Li, M. Yang, J.-S. Park, S.-H. Wei, J. J. Berry, K. Zhu, *Chem. Mater.* **2016**, *28*, 284.
[45] C. Yi, J. Luo, S. Meloni, A. Boziki, N. Ashari-Astani, C. Grätzel, S. M. Zakeeruddin, U. Röthlisberger, M. Grätzel, *Energy Environ. Sci.* **2016**, *9*, 656.
[46] Y. Zhao, K. Zhu, *Chem. Soc. Rev.* **2016**, *45*, 655.
[47] G. Kieslich, S. Sun, A. K. Cheetham, *Chem. Sci.* **2014**, *5*, 4712.

[48] J. H. Noh, S. H. Im, J. H. Heo, T. N. Mandal, S. Il Seok, *Nano Lett.* **2013**, *13*, 1764.
[49] P. Tyagi, L. Indu Giri, S. Tuli, R. Srivastava, *J. Appl. Phys.* **2014**, *115*, 34518.
[50] J. Park, H. Ham, C. Park, *Org. Electron.* **2011**, *12*, 227.
[51] K. Qasim, B. Wang, Y. Zhang, P. Li, Y. Wang, S. Li, S.-T. Lee, L.-S. Liao, W. Lei, Q. Bao, *Adv. Funct. Mater.* **2017**, *27*, 1606874.
[52] L. Zhao, J. Gao, Y. L. Lin, Y.-W. Yeh, K. M. Lee, N. Yao, Y.-L. Loo, B. P. Rand, *Adv. Mater.* **2017**, *29*, 1605317.
[53] E. J. Juarez-Perez, Z. Hawash, S. R. Raga, L. K. Ono, Y. Qi, *Energy Environ. Sci.* **2016**, *9*, 3406.
[54] B. Brunetti, C. Cavallo, A. Ciccioli, G. Gigli, A. Latini, *Sci. Rep.* **2016**, *6*, 31896.
[55] A. Latini, G. Gigli, A. Ciccioli, *Sustainable Energy Fuels* **2017**, *1*, 1351.
[56] M. Kulbak, S. Gupta, N. Kedem, I. Levine, T. Bendikov, G. Hodes, D. Cahen, *J. Phys. Chem. Lett.* **2016**, *7*, 167.
[57] A. Dualeh, P. Gao, S. Il Seok, M. K. Nazeeruddin, M. Grätzel, *Chem. Mater.* **2014**, *26*, 6160.
[58] Z. Song, S. C. Watthage, A. B. Phillips, B. L. Tompkins, R. J. Ellingson, M. J. Heben, *Chem. Mater.* **2015**, *27*, 4612.
[59] A. Dualeh, N. Tétreault, T. Moehl, P. Gao, M. K. Nazeeruddin, M. Grätzel, *Adv. Funct. Mater.* **2014**, *24*, 3250.
[60] T. Supasai, N. Rujisamphan, K. Ullrich, A. Chemseddine, T. Dittrich, *Appl. Phys. Lett.* **2013**, *103*, 183906.
[61] B. Conings, J. Drijkoningen, N. Gauquelin, A. Babayigit, J. D'Haen, L. D'Olieslaeger, A. Ethirajan, J. Verbeeck, J. Manca, E. Mosconi, F. De Angelis, H.-G. Boyen, *Adv. Energy Mater.* **2015**, *5*, 1500477.
[62] Y.-H. Kim, H. Cho, J. H. Heo, S. H. Im, T.-W. Lee, *Curr. Appl. Phys.* **2016**, *16*, 1069.
[63] R. K. Misra, S. Aharon, B. Li, D. Mogilyansky, I. Visoly-Fisher, L. Etgar, E. A. Katz, *J. Phys. Chem. Lett.* **2015**, *6*, 326.
[64] G. P. Nagabhushana, R. Shivaramaiah, A. Navrotsky, *Proc. Natl. Acad. Sci. USA* **2016**, *113*, 7717.
[65] A. Buin, R. Comin, J. Xu, A. H. Ip, E. H. Sargent, *Chem. Mater.* **2015**, *27*, 4405.
[66] C. Müller, T. Glaser, M. Plogmeyer, M. Sendner, S. Döring, A. A. Bakulin, C. Brzuska, R. Scheer, M. S. Pshenichnikov, W. Kowalsky, A. Pucci, R. Lovrinčić, *Chem. Mater.* **2015**, *27*, 7835.
[67] K. K. Bass, R. E. Mcanally, S. Zhou, P. I. Djurovich, M. E. Thompson, B. C. Melot, *Chem. Commun.* **2014**, *50*, 15819.
[68] J. Yang, T. L. Kelly, *Inorg. Chem.* **2017**, *56*, 92.
[69] M. K. Gangishetty, R. W. J. Scott, T. L. Kelly, *Nanoscale* **2016**, *8*, 6300.
[70] H. P. Zhou, Q. Chen, G. Li, S. Luo, T. B. Song, H. S. Duan, Z. R. Hong, J. B. You, Y. S. Liu, Y. Yang, *Science* **2014**, *345*, 542.
[71] L. Zhang, M. Ju, W. Liang, *Phys. Chem. Chem. Phys.* **2016**, *18*, 23174.
[72] S. N. Habisreutinger, T. Leijtens, G. E. Eperon, S. D. Stranks, R.J. Nicholas, H. J. Snaith, *Nano Lett.* **2014**, *14*, 5561.
[73] J. Li, X. Shan, S. G. R. Bade, T. Geske, Q. Jiang, X. Yang, Z. Yu, *J. Phys. Chem. Lett.* **2016**, *7*, 4059.
[74] Q. Shan, J. Li, J. Song, Y. Zou, L. Xu, J. Xue, Y. Dong, C. Huo, J. Chen, B. Han, H. Zeng, *J. Mater. Chem. C* **2017**, *5*, 4565.
[75] S. N. Habisreutinger, D. P. McMeekin, H. J. Snaith, R. J. Nicholas, *APL Mater.* **2016**, *4*, 91503.
[76] N. Aristidou, I. Sanchez-Molina, T. Chotchuangchutchaval, M. Brown, L. Martinez, T. Rath, S. A. Haque, *Angew. Chem., Int. Ed.* **2015**, *54*, 8208.
[77] K. Momma, F. Izumi, *J. Appl. Crystallogr.* **2011**, *44*, 1272.
[78] Y. Tian, M. Peter, E. Unger, M. Abdellah, K. Zheng, T. Pullerits, A. Yartsev, V. Sundström, I. G. Scheblykin, *Phys. Chem. Chem. Phys.* **2015**, *17*, 24978.
[79] N. Aristidou, C. Eames, I. Sanchez-Molina, X. Bu, J. Kosco, M. S. Islam, S. A. Haque, *Nat. Commun.* **2017**, *8*, 15218.
[80] S. Huang, Z. Li, B. Wang, N. Zhu, C. Zhang, L. Kong, Q. Zhang, A. Shan, L. Li, *ACS Appl. Mater. Interfaces* **2017**, *9*, 7249.
[81] S. G. Motti, M. Gandini, A. J. Barker, J. M. Ball, A. R. Srimath Kandada, A. Petrozza, *ACS Energy Lett.* **2016**, *1*, 726.
[82] N. K. Noel, A. Abate, S. D. Stranks, E. S. Parrott, V. M. Burlakov, A. Goriely, H. J. Snaith, *ACS Nano* **2014**, *8*, 9815.
[83] J. W. Lee, H. S. Kim, N. G. Park, *Acc. Chem. Res.* **2016**, *49*, 311.
[84] J. Kim, S. Lee, J. H. Lee, K.-H. Hong, *J. Phys. Chem. Lett.* **2014**, *5*, 1312.
[85] J.-W. Lee, D.-H. Kim, H.-S. Kim, S.-W. Seo, S. M. Cho, N.-G. Park, *Adv. Energy Mater.* **2015**, *5*, 1501310.
[86] L. Zhao, R. A. Kerner, Z. Xiao, Y. L. Lin, K. M. Lee, J. Schwartz, B. P. Rand, *ACS Energy Lett.* **2016**, *1*, 595.
[87] N. A. Manshor, Q. Wali, K. K. Wong, S. K. Muzakir, A. Fakharuddin, L. Schmidt-Mende, R. Jose, *Phys. Chem. Chem. Phys.* **2016**, *18*, 21629.
[88] D. Bryant, N. Aristidou, S. Pont, I. Sanchez-Molina, T. Chotchuna ngatchaval, S. Wheeler, J. R. Durrant, S. A. Haque, *Energy Environ. Sci.* **2016**, *9*, 1655.
[89] M. E. Vaida, R. Tchitnga, T. M. Bernhardt, *Beilstein J. Nanotechnol.* **2011**, *2*, 618.
[90] S. Wang, Y. Jiang, E. J. Juarez-Perez, L. K. Ono, Y. Qi, *Nat. Energy* **2016**, *2*, 16195.
[91] G. Grancini, C. Roldán-Carmona, I. Zimmermann, E. Mosconi, X. Lee, D. Martineau, S. Narbey, F. Oswald, F. De Angelis, M. Graetzel, M. K. Nazeeruddin, *Nat. Commun.* **2017**, *8*, 15684.
[92] Y. Yang, M. Yang, Z. Li, R. Crisp, K. Zhu, M. C. Beard, *J. Phys. Chem. Lett.* **2015**, *6*, 4688.
[93] R. L. Milot, R. J. Sutton, G. E. Eperon, A. A. Haghighirad, J. Martinez Hardigree, L. Miranda, H. J. Snaith, M. B. Johnston, L. M. Herz, *Nano Lett.* **2016**, *16*, 7001.
[94] F. Deschler, M. Price, S. Pathak, L. E. Klintberg, D. D. Jarausch, R. Higler, S. Hüttner, T. Leijtens, S. D. Stranks, H. J. Snaith, M. Atatüre, R. T. Phillips, R. H. Friend, *J. Phys. Chem. Lett.* **2014**, *5*, 1421.
[95] Y. Rakita, S. R. Cohen, N. K. Kedem, G. Hodes, D. Cahen, *MRS Commun.* **2015**, *5*, 623.
[96] M. Cadelano, V. Sarritzu, N. Sestu, D. Marongiu, F. Chen, R. Piras, R. Corpino, C. M. Carbonaro, F. Quochi, M. Saba, A. Mura, G. Bongiovanni, *Adv. Opt. Mater.* **2015**, *3*, 1557.
[97] F. Zhang, H. Zhong, C. Chen, X. Wu, X. Hu, H. Huang, J. Han, B. Zou, Y. Dong, *ACS Nano* **2015**, *9*, 4533.
[98] X. Li, Y. Wu, S. Zhang, B. Cai, Y. Gu, J. Song, H. Zeng, *Adv. Funct. Mater.* **2016**, *26*, 2435.
[99] L. C. Schmidt, A. Pertegás, S. González-Carrero, O. Malinkiewicz, S. Agouram, G. M. Espallargas, H. J. Bolink, R. E. Galian, J. Peréz-Prieto, *J. Am. Chem. Soc.* **2014**, *136*, 850.
[100] M. F. Aygüler, M. D. Weber, B. M. D. Puscher, D. D. Medina, P. Docampo, R. D. Costa, *J. Phys. Chem. C* **2015**, *119*, 12047.
[101] J. Li, L. Xu, T. Wang, J. Song, J. Chen, J. Xue, Y. Dong, B. Cai, Q. Shan, B. Han, H. Zeng, *Adv. Mater.* **2017**, *29*, 1603885.
[102] X. Zhang, C. Sun, Y. Zhang, H. Wu, C. Ji, Y. Chuai, P. Wang, S. Wen, C. Zhang, W. W. Yu, *J. Phys. Chem. Lett.* **2016**, *7*, 4602.
[103] J. Song, J. Li, X. Li, L. Xu, Y. Dong, H. Zeng, *Adv. Mater.* **2015**, *27*, 7162.
[104] I. Levchuk, A. Osvet, X. Tang, M. Brandl, J. D. Perea, F. Hoegl, G. J. Matt, R. Hock, M. Batentschuk, C. J. Brabec, *Nano Lett.* **2017**, *17*, 2765.
[105] L. Protesescu, S. Yakunin, M. I. Bodnarchuk, F. Bertolotti, N. Masciocchi, A. Guagliardi, M. V. Kovalenko, *J. Am. Chem. Soc.* **2016**, *138*, 14202.
[106] E.-P. Yao, Z. Yang, L. Meng, P. Sun, S. Dong, Y. Yang, Y. Yang, *Adv. Mater.* **2017**, *29*, 1606859.
[107] B. Luo, Y.-C. Pu, S. A. Lindley, Y. Yang, L. Lu, Y. Li, X. Li, J. Z. Zhang, *Angew. Chem., Int. Ed.* **2016**, *128*, 9010.

[108] Y. Wang, J. He, H. Chen, J. Chen, R. Zhu, P. Ma, A. Towers, Y. Lin, A. J. Gesquiere, S.-T. Wu, Y. Dong, *Adv. Mater.* **2016**, *28*, 10710.
[109] J. Pan, L. N. Quan, Y. Zhao, W. Peng, B. Murali, S. P. Sarmah, M. Yuan, L. Sinatra, N. M. Alyami, J. Liu, E. Yassitepe, Z. Yang, O. Voznyy, R. Comin, M. N. Hedhili, O. F. Mohammed, Z. H. Lu, D. H. Kim, E. H. Sargent, O. M. Bakr, *Adv. Mater.* **2016**, *28*, 8718.
[110] W. Deng, X. Xu, X. Zhang, Y. Zhang, X. Jin, L. Wang, S.-T. Lee, J. Jie, *Adv. Funct. Mater.* **2016**, *26*, 4797.
[111] Y. Ling, Z. Yuan, Y. Tian, X. Wang, J. C. Wang, Y. Xin, K. Hanson, B. Ma, H. Gao, *Adv. Mater.* **2016**, *28*, 305.
[112] Z. Wei, A. Perumal, R. Su, S. Sushant, J. Xing, Q. Zhang, S. T. Tan, H. V. Demir, Q. Xiong, *Nanoscale* **2016**, *8*, 18021.
[113] Y. Yuan, J. Huang, *Acc. Chem. Res.* **2016**, *49*, 286.
[114] H. Back, G. Kim, J. Kim, J. Kong, T. K. Kim, H. Kang, H. Kim, J. Lee, S. Lee, K. Lee, *Energy Environ. Sci.* **2016**, *9*, 1258.
[115] C. Besleaga, L. E. Abramiuc, V. Stancu, A. G. Tomulescu, M. Sima, L. Trinca, N. Plugaru, L. Pintilie, G. A. Nemnes, M. Iliescu, H. G. Svavarsson, A. Manolescu, I. Pintilie, *J. Phys. Chem. Lett.* **2016**, *7*, 5168.
[116] J. Carrillo, A. Guerrero, S. Rahimnejad, O. Almora, I. Zarazua, E. Mas-Marza, J. Bisquert, G. Garcia-Belmonte, *Adv. Energy Mater.* **2016**, *6*, 1502246.
[117] N. Ahn, K. Kwak, M. S. Jang, H. Yoon, B. Y. Lee, J. Lee, P. V. Pikhitsa, J. Byun, M. Choi, *Nat. Commun.* **2016**, *7*, 13422.
[118] J. Li, S. G. R. Bade, X. Shan, Z. Yu, *Adv. Mater.* **2015**, *27*, 5196.
[119] X. Shan, J. Li, M. Chen, T. Geske, S. G. R. Bade, Z. Yu, *J. Phys. Chem. Lett.* **2017**, *8*, 2412.
[120] X. Wang, Y. Ling, Y.-C. Chiu, Y. Du, J. L. Barreda, F. Perez-Orive, B. Ma, P. Xiong, H. Gao, *Nano Lett.* **2017**, *17*, 4831.
[121] Y. Shao, Y. Fang, T. Li, Q. Wang, Q. Dong, Y. Deng, Y. Yuan, H. Wei, M. Wang, A. Gruverman, J. Shield, J. Huang, *Energy Environ. Sci.* **2016**, *9*, 1752.
[122] J. Schoonman, *J. Solid State Chem.* **1972**, *4*, 466.
[123] J. M. Azpiroz, E. Mosconi, J. Bisquert, F. De Angelis, *Energy Environ. Sci.* **2015**, *8*, 2118.
[124] J. Haruyama, K. Sodeyama, L. Han, Y. Tateyama, *J. Am. Chem. Soc.* **2015**, *137*, 10048.
[125] C. Eames, J. M. Frost, P. R. F. Barnes, B. C. O'Regan, A. Walsh, M. S. Islam, *Nat. Commun.* **2015**, *6*, 7497.
[126] J. Mizusaki, K. Arai, K. Fueki, *Solid State Ionics* **1983**, *11*, 203.
[127] A. Senocrate, I. Moudrakovski, G. Y. Kim, T.-Y. Yang, G. Gregori, M. Grätzel, J. Maier, *Angew. Chem., Int. Ed.* **2017**, *56*, 7755.
[128] S. Chen, X. Wen, R. Sheng, S. Huang, X. Deng, M. A. Green, A. Ho-Baillie, *ACS Appl. Mater. Interfaces* **2016**, *8*, 5351.
[129] E. Bi, H. Chen, F. Xie, Y. Wu, W. Chen, Y. Su, A. Islam, M. Grätzel, X. Yang, L. Han, *Nat. Commun.* **2017**, *8*, 15330.
[130] L. Zhang, X. Yang, Q. Jiang, P. Wang, Z. Yin, X. Zhang, H. Tan, Y. M. Yang, M. Wei, B. R. Sutherland, E. H. Sargent, J. You, *Nat. Commun.* **2017**, *8*, 15640.
[131] J. Si, Y. Liu, N. Wang, M. Xu, J. Li, H. He, J. Wang, Y. Jin, *Nano Res.* **2017**, *10*, 1329.
[132] Y. Shao, G. C. Bazan, A. J. Heeger, *Adv. Mater.* **2007**, *19*, 365.
[133] Z. Yu, M. Wang, G. Lei, J. Liu, L. Li, Q. Pei, *J. Phys. Chem. Lett.* **2011**, *2*, 367.
[134] S. van Reenen, P. Matyba, A. Dzwilewski, R. A. J. Janssen, L. Edman, M. Kemerink, *J. Am. Chem. Soc.* **2010**, *132*, 13776.
[135] V. Bychkov, P. Matyba, V. Akkerman, M. Modestov, D. Valiev, G. Brodin, C. K. Law, M. Marklund, L. Edman, *Phys. Rev. Lett.* **2011**, *107*, 16103.
[136] S. Tang, L. Edman, *Top. Curr. Chem.* **2016**, *374*, 40.
[137] T. Wågberg, P. R. Hania, N. D. Robinson, J. H. Shin, P. Matyba, L. Edman, *Adv. Mater.* **2008**, *20*, 1744.
[138] S. Van Reenen, P. Matyba, A. Dzwilewski, R. A. J. Janssen, L. Edman, M. Kemerink, *Adv. Funct. Mater.* **2011**, *21*, 1795.
[139] H. Zhang, H. Lin, C. Liang, H. Liu, J. Liang, Y. Zhao, W. Zhang, M. Sun, W. Xiao, H. Li, S. Polizzi, D. Li, F. Zhang, Z. He, W. C. H. Choy, *Adv. Funct. Mater.* **2015**, *25*, 7226.
[140] Z. Xiao, Y. Yuan, Y. Shao, Q. Wang, Q. Dong, C. Bi, P. Sharma, A. Gruverman, J. Huang, *Nat. Mater.* **2015**, *14*, 193.
[141] K. Domanski, J. P. Correa-Baena, N. Mine, M. K. Nazeeruddin, A. Abate, M. Saliba, W. Tress, A. Hagfeldt, M. Grätzel, *ACS Nano* **2016**, *10*, 6306.
[142] R. Sheng, A. Ho-Baillie, S. Huang, S. Chen, X. Wen, X. Hao, M. A. Green, *J. Phys. Chem. C* **2015**, *119*, 3545.
[143] O. V. Mikhnenko, P. W. M. Blom, T.-Q. Nguyen, *Energy Environ. Sci.* **2015**, *8*, 1867.
[144] P. Vashishtha, J. E. Halpert, *Chem. Mater.* **2017**, *29*, 5965.
[145] G. Li, F. W. R. Rivarola, N. J. L. K. Davis, S. Bai, T. C. Jellicoe, F. De La Peña, S. Hou, C. Ducati, F. Gao, R. H. Friend, N. C. Greenham, Z. K. Tan, *Adv. Mater.* **2016**, *28*, 3528.
[146] F. Brivio, C. Caetano, A. Walsh, *J. Phys. Chem. Lett.* **2016**, *7*, 1083.
[147] C. G. Bischak, C. L. Hetherington, H. Wu, S. Aloni, D. F. Ogletree, D. T. Limmer, N. S. Ginsberg, *Nano Lett.* **2017**, *17*, 1028.
[148] Z.-Q. Zhu, K. Klimes, S. Holloway, J. Li, *Adv. Mater.* **2017**, *29*, 1605002.
[149] C. Wu, Y. Zou, T. Wu, M. Ban, V. Pecunia, Y. Han, Q. Liu, T. Song, S. Duhm, B. Sun, *Adv. Funct. Mater.* **2017**, *27*, 1700338.
[150] H. Sun, Z. Yang, M. Wei, W. Sun, X. Li, S. Ye, Y. Zhao, H. Tan, E. L. Kynaston, T. B. Schon, H. Yan, Z.-H. Lu, G. A. Ozin, E. H. Sargent, D. S. Seferos, *Adv. Mater.* **2017**, *29*, 1701153.
[151] J. C. Yu, D. B. Kim, G. Baek, B. R. Lee, E. D. Jung, S. Lee, J. H. Chu, D. K. Lee, K. J. Choi, S. Cho, M. H. Song, *Adv. Mater.* **2015**, *27*, 3492.
[152] N. Yantara, S. Bhaumik, F. Yan, D. Sabba, H. A. Dewi, N. Mathews, P. P. Boix, H. V. Demir, S. Mhaisalkar, *J. Phys. Chem. Lett.* **2015**, *6*, 4360.
[153] X. Zhang, H. Lin, H. Huang, C. Reckmeier, Y. Zhang, W. C. H. Choy, A. L. Rogach, *Nano Lett.* **2016**, *16*, 1415.
[154] J. C. Yu, D. W. Kim, D. B. Kim, E. D. Jung, J. H. Park, A.-Y. Lee, B. R. Lee, D. Di Nuzzo, R. H. Friend, M. H. Song, *Adv. Mater.* **2016**, *28*, 6906.
[155] H. Hu, T. Salim, B. Chen, Y. M. Lam, *Sci. Rep.* **2016**, *6*, 33546.
[156] Z. Shi, Y. Li, Y. Zhang, Y. Chen, X. Li, D. Wu, T. Xu, C. Shan, G. Du, *Nano Lett.* **2017**, *17*, 313.
[157] H. P. Kim, J. Kim, B. S. Kim, H. M. Kim, J. Kim, A. R. bin Mohd Yusoff, J. Jang, M. K. Nazeeruddin, *Adv. Opt. Mater.* **2017**, *5*, 1600920.
[158] X. Zhang, H. Liu, W. Wang, J. Zhang, B. Xu, K. L. Karen, Y. Zheng, S. Liu, S. Chen, K. Wang, X. W. Sun, *Adv. Mater.* **2017**, *29*, 1606405.
[159] J. C. Yu, A.-Y. Lee, D. B. Kim, E. D. Jung, D. W. Kim, M. H. Song, *Adv. Mater. Technol.* **2017**, *2*, 1700003.
[160] S. Zhang, C. Yi, N. Wang, Y. Sun, W. Zou, Y. Wei, Y. Cao, Y. Miao, R. Li, Y. Yin, N. Zhao, J. Wang, W. Huang, *Adv. Mater.* **2017**, *29*, 1606600.
[161] X. Zhang, W. Wang, B. Xu, S. Liu, H. Dai, D. Bian, S. Chen, K. Wang, X. W. Sun, *Nano Energy* **2017**, *37*, 40.
[162] M. Chen, X. Shan, T. Geske, J. Li, Z. Yu, *ACS Nano* **2017**, *11*, 6312.
[163] Y. Hu, Q. Wang, Y.-L. Shi, M. Li, L. Zhang, Z.-K. Wang, L.-S. Liao, *J. Mater. Chem. C* **2017**, *5*, 8144.
[164] F. C. Hanusch, E. Wiesenmayer, E. Mankel, A. Binek, P. Angloher, C. Fraunhofer, N. Giesbrecht, J. M. Feckl, W. Jaegermann, D. Johrendt, T. Bein, P. Docampo, *J. Phys. Chem. Lett.* **2014**, *5*, 2791.
[165] A. Amat, E. Mosconi, E. Ronca, C. Quarti, P. Umari, M. K. Nazeeruddin, M. Grätzel, F. De Angelis, *Nano Lett.* **2014**, *14*, 3608.
[166] L. Meng, E.-P. Yao, Z. Hong, H. Chen, P. Sun, Z. Yang, G. Li, Y. Yang, *Adv. Mater.* **2017**, *29*, 1603826.

[167] A. Perumal, S. Shendre, M. Li, Y. K. E. Tay, V. K. Sharma, S. Chen, Z. Wei, Q. Liu, Y. Gao, P. J. S. Buenconsejo, S. T. Tan, C. L. Gan, Q. Xiong, T. C. Sum, H. V. Demir, *Sci. Rep.* **2016**, *6*, 36733.
[168] D. Shi, V. Adinolfi, R. Comin, M. Yuan, E. Alarousu, A. Buin, Y. Chen, S. Hoogland, A. Rothenberger, K. Katsiev, Y. Losovyj, X. Zhang, P. A. Dowben, O. F. Mohammed, E. H. Sargent, O. M. Bakr, *Science* **2015**, *347*, 519.
[169] L. Atourki, E. Vega, M. Mollar, B. Marí, H. Kirou, K. Bouabid, A. Ihlal, *J. Alloys Compd.* **2017**, *702*, 404.
[170] A. Swarnkar, R. Chulliyil, V. K. Ravi, M. Irfanullah, A. Chowdhury, A. Nag, *Angew. Chem., Int. Ed.* **2015**, *54*, 15424.
[171] W. Rehman, D. P. McMeekin, J. B. Patel, R. L. Milot, M. B. Johnston, H. J. Snaith, L. M. Herz, *Energy Environ. Sci.* **2017**, *10*, 361.
[172] O. A. Syzgantseva, M. Saliba, M. Grätzel, U. Rothlisberger, *J. Phys. Chem. Lett.* **2017**, *8*, 1191.
[173] M. Saliba, T. Matsui, K. Domanski, J.-Y. Seo, A. Ummadisingu, S. M. Zakeeruddin, J.-P. Correa-Baena, W. R. Tress, A. Abate, A. Hagfeldt, M. Grätzel, *Science* **2016**, *354*, 206.
[174] X. Hong, T. Ishihara, A. V. Nurmikko, *Phys. Rev. B* **1992**, *45*, 6961.
[175] B.-E. Cohen, M. Wierzbowska, L. Etgar, *Adv. Funct. Mater.* **2017**, *27*, 1604733.
[176] O. Yaffe, A. Chernikov, Z. M. Norman, Y. Zhong, A. Velauthapillai, A. van der Zande, J. S. Owen, T. F. Heinz, *Phys. Rev. B* **2015**, *92*, 45414.
[177] T. Goto, H. Makino, T. Yao, C. H. Chia, T. Makino, Y. Segawa, G. A. Mousdis, G. C. Papavassiliou, *Phys. Rev. B* **2006**, *73*, 115206.
[178] I. B. Koutselas, L. Ducasse, G. C. Papavassiliou, *J. Phys.: Condens. Matter* **1999**, *8*, 1217.
[179] K. Tanaka, T. Takahashi, T. Ban, T. Kondo, K. Uchida, N. Miura, *Solid State Commun.* **2003**, *127*, 619.
[180] G. Xing, B. Wu, X. Wu, M. Li, B. Du, Q. Wei, J. Guo, E. K. L. Yeow, T. C. Sum, W. Huang, *Nat. Commun.* **2017**, *8*, 14558.
[181] L. N. Quan, M. Yuan, R. Comin, O. Voznyy, E. M. Beauregard, S. Hoogland, A. Buin, A. R. Kirmani, K. Zhao, A. Amassian, D. H. Kim, E. H. Sargent, *J. Am. Chem. Soc.* **2016**, *138*, 2649.
[182] Z. Chen, C. Zhang, X.-F. Jiang, M. Liu, R. Xia, T. Shi, D. Chen, Q. Xue, Y.-J. Zhao, S. Su, H.-L. Yip, Y. Cao, *Adv. Mater.* **2017**, *29*, 1603157.
[183] L. Cheng, Y. Cao, R. Ge, Y.-Q. Wei, N.-N. Wang, J.-P. Wang, W. Huang, *Chin. Chem. Lett.* **2017**, *28*, 29.
[184] M. Wei, W. Sun, Y. Liu, Z. Liu, L. Xiao, Z. Bian, Z. Chen, *Phys. Status Solidi A* **2016**, *213*, 2727.
[185] K. O. Brinkmann, J. Zhao, N. Pourdavoud, T. Becker, T. Hu, S. Olthof, K. Meerholz, L. Hoffmann, T. Gahlmann, R. Heiderhoff, M. F. Oszajca, N. A. Luechinger, D. Rogalla, Y. Chen, B. Cheng, T. Riedl, *Nat. Commun.* **2017**, *8*, 13938.
[186] A. Behrendt, C. Friedenberger, T. Gahlmann, S. Trost, T. Becker, K. Zilberberg, A. Polywka, P. Görrn, T. Riedl, *Adv. Mater.* **2015**, *27*, 5961.
[187] T.-W. Lee, M.-G. Kim, S. H. Park, S. Y. Kim, O. Kwon, T. Noh, J.-J. Park, T.-L. Choi, J. H. Park, B. D. Chin, *Adv. Funct. Mater.* **2009**, *19*, 1863.
[188] T.-W. Lee, Y. Chung, O. Kwon, J.-J. Park, *Adv. Funct. Mater.* **2007**, *17*, 390.
[189] Y. Zhao, J. Wei, H. Li, Y. Yan, W. Zhou, D. Yu, Q. Zhao, *Nat. Commun.* **2016**, *7*, 10228.
[190] Z. Liu, J. Hu, H. Jiao, L. Li, G. Zheng, Y. Chen, Y. Huang, Q. Zhang, C. Shen, Q. Chen, H. Zhou, *Adv. Mater.* **2017**, *29*, 1606774.
[191] H. Huang, H. Lin, S. V. Kershaw, A. S. Susha, W. C. H. Choy, A. L. Rogach, *J. Phys. Chem. Lett.* **2016**, *7*, 4398.
[192] Q. Zhou, Z. Bai, W.-G. Lu, Y. Wang, B. Zou, H. Zhong, *Adv. Mater.* **2016**, *28*, 9163.
[193] Y. H. Song, S. H. Choi, J. S. Yoo, B. K. Kang, E. K. Ji, H. S. Jung, D. H. Yoon, *Chem. Eng. J.* **2017**, *313*, 461.
[194] T.-W. Lee, T. Noh, H.-W. Shin, O. Kwon, J.-J. Park, B.-K. Choi, M.-S. Kim, D. W. Shin, Y.-R. Kim, *Adv. Funct. Mater.* **2009**, *19*, 1625.
[195] T. Miyadera, T. Sugita, H. Tampo, K. Matsubara, M. Chikamatsu, *ACS Appl. Mater. Interfaces* **2016**, *8*, 26013.
[196] Y. Chen, Y. Xia, G. M. Smith, D. L. Carroll, *Adv. Mater.* **2014**, *26*, 8133.
[197] S. H. Cho, S. S. Jo, I. Hwang, J. Sung, J. Seo, S.-H. Jung, I. Bae, J. R. Choi, H. Cho, T. Lee, J. K. Lee, T.-W. Lee, C. Park, *ACS Nano* **2013**, *7*, 10809.
[198] C.-L. Lin, C.-C. Hung, P.-Y. Kuo, M.-H. Cheng, *J. Disp. Technol.* **2012**, *8*, 681.
[199] S. Pathak, N. Sakai, F. W. R. Rivarola, S. D. Stranks, J. Liu, G. E. Eperon, C. Ducati, K. Wojciechowski, J. T. Griffiths, A. A. Haghighirad, A. Pellaroque, R. H. Friend, H. J. Snaith, *Chem. Mater.* **2015**, *27*, 8066.

